# Chapter 1

# Introduction

## 1.1 Historical development

The use of water to reduce the environmental temperature is not an innovative technique. Reports in the history of the architecture and the old civilizations prove the presence of water fountains, vegetation and cascades in patios. Room openings facing these patios contribute to reduce hostility of hot and dry air in the interior of the residences. Public buildings with higher occupation, such as palaces, schools and mosques also incorporated this technique. In the typical mosque architecture, there is a great patio with central fountain for the religion ritual. Moreover religious significances, the water also provides maintenance of the internal microclimate of the mosque. In modern architecture, the evaporative cooling is regarded having in mind the development of air conditioning industry. In the post-war period, the evaporative cooling as a technique for environmental conditioning has developed with new materials and noise attenuation, the contribution of air-conditioning machines. The evaporative cooling is a passive method that can save the fossils fuel reserves or contribute to prevent the use of gas CFC in the refrigeration, one of the possible causes of the global heating. Much of the post-harvest loss of fruits and vegetables in developing countries is due to the lack of proper storage facilities. While refrigerated cool stores are the best method of preserving fruits and vegetables they are expensive to buy and run. Consequently, in developing countries there is an interest in simple low-cost alternatives, many of which depend on evaporative cooling which is simple and does not require any external power supply. The basic principle relies on cooling by evaporation. When water evaporates it draws energy from its surroundings which produce a considerable cooling effect. Evaporative cooling occurs when air, that is not too humid, passes over a wet surface; the faster the rate of evaporation the greater the cooling.

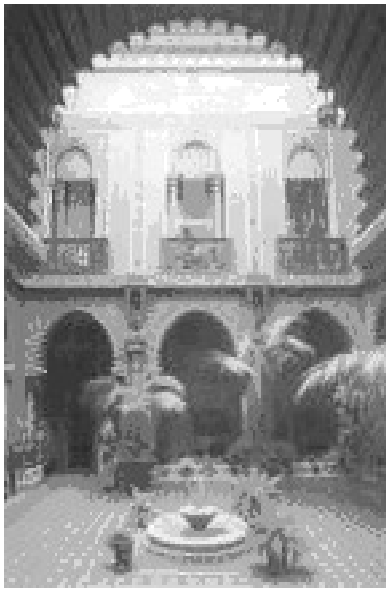

**Figure 1.1 Opening facing a patio**

**Figure 1.2 Water fountain and vegetation in Arab residential patio**

The efficiency of an evaporative cooler depends on the humidity of the surrounding air. Very dry air can absorb a lot of moisture so greater cooling occurs. In the extreme case of air that is totally saturated with water, no evaporation can take place and no cooling occurs. Generally, an evaporative cooler is made of a porous material that is fed with water. Hot dry air is drawn over the material. The water evaporates into the air raising its humidity and at the same time reducing the temperature of the air. There are many different styles of evaporative coolers. The design will depend on the materials available and the user's requirements. Some examples of evaporative cooling designs are described below.

## Pot designs

These are simple designs of evaporative coolers that can be used in the home. The basic design consists of a storage pot placed inside a bigger pot that holds water. The inner pot stores food that is kept cool. One adaptation on the basic double pot design is the Janata cooler, developed by the Food & Nutrition Board of India. A storage pot is placed in an earthenware bowl containing water. The pot is then covered with a damp cloth that is dipped into the reservoir of water. Water drawn up the cloth evaporates keeping the storage pot cool. The bowl is also placed on wet sand, to isolate the pot from the hot ground. Mohammed Bah

Abba a teacher in Nigeria developed a small-scale storage “pot-in-pot” system that uses two pots of slightly different size. The smaller pot is placed inside the larger pot and the gap between the two pots is filled with sand. Mohammed won the Rolex 200 Award for Enterprise for his design. In Sudan, Practical Action and the Woman’s Association for Earthenware Manufacturing have been experimenting with the storage design of Mohammed Bah Abba. The aim of the experimentation was to discover how effective and economical the Zeer storage is in conserving foods. Zeer is the Arabic name for the large pots used. The results are shown in Figure Janata Cooler

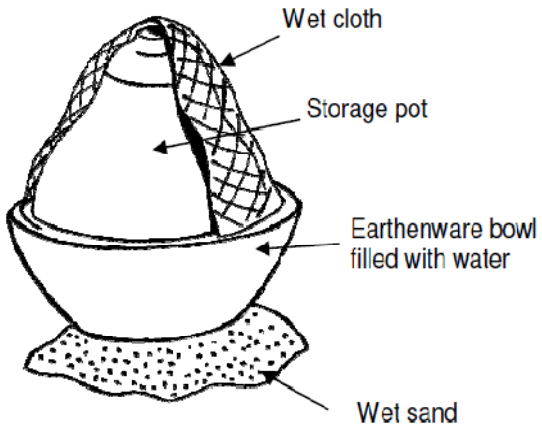


**Figure 1.3 Janata Cooler**

In a bamboo cooler base of the cooler is made from a large diameter tray that contains water. Bricks are placed within this tray and an open weave cylinder of bamboo or similar material is placed on top of the bricks. Hessian cloth is wrapped around the bamboo frame, ensuring that the cloth is dipping into the water to allow water to be drawn up the cylinder’s wall. Food is kept in the cylinder with a lid placed on the top.

An almirah cooler is a more sophisticated cooler that has a wooden frame covered in cloth. There is a water tray at the base and on top of the frame into which the cloth dips, thus keeping it wet. A hinged door and internal shelves allow easy access to the stored produce.

The charcoal cooler is made from an open timber frame of approximately 50mm x 25mm (2” x 1”) in section. The door is made by simply hinging one side of the frame. The wooden

frame is covered in mesh, inside and out, leaving a 25mm (1”) cavity which is filled with pieces of charcoal. The charcoal is sprayed with water, and when wet provides evaporative cooling. The framework is mounted outside the house on a pole with a metal cone to deter rats and a good coating of grease to prevent ants getting to the food. The top is usually solid and thatched, with an overhang to deter flying insects. All cooling chambers should be placed in a shady position, and exposure to the wind will help the cooling effect. Airflows can be artificially created through the use of a chimney. For example using a mini electric fan or an oil lamp to create airflows through the chimney - the resulting draft draws cooler air into the cabinet situated below the chimney. The Bhartya cool cabinet uses this principle to keep its contents cool. Wire mesh shelves and holes in the bottom of the raised cabinet ensure the free movement of air passing over the stored food.

## 1.2 The evaporative cooling technique

Evaporative cooling occurs when moisture is added to air that has a relative humidity of less than 100 percent. The lower the relative humidity, the greater the temperature drops when moisture is added. The technology is a versatile and energy-efficient alternative or adjunct to compressor-based cooling. In favourable climates (most of the northern and north-western India and other dry-climate areas worldwide), evaporative cooling can fully satisfy building cooling loads using one-fourth the energy of conventional equipment. It can also be applied cost-effectively when integrated with conventional chillers’ systems. Using evaporative technology can also improve a facility load profile, which can enhance a company's negotiating position in a retail electricity market.

Evaporative cooling systems, such as water cooling towers, evaporative condensers, evaporative fluid coolers, air washers and dehumidifying coils are widely used all around us. Their key process is heat and moisture transfer between air and water. The use of evaporation of water in air conditioning is an old and much known technology. However its importance is

again being recognized due to characteristics of zero pollution, energy efficiency, simplicity and good indoor air quality. Evaporative cooling process remains one of the least expensive techniques to bring dry bulb temperature to more comfortable range and has been used to improve human comfort conditions since a long time in the thermal environmental control applications. The principle of evaporative cooling indicates that the evaporative cooling system can only remove sensible heat, thus the evaporative cooling system works best in hot and dry climate where the maximum evaporative cooling will result. Evaporative cooling occurs when moisture is added to air that has relative humidity less than 100%. The lower the relative humidity, which is dependent on the airs dry and wet bulb temperatures, the greater the potential for evaporative cooling. The cooling sensation felt by a person breeze passes over and evaporates perspiration on the skin, is doubtless the most common human experience with the phenomenon.

All humidification systems that use liquid involve an exchange between the latent heat and the sensible heat in the air stream: the latent heat portion increases, the sensible portion decreases. For an essentially unvaried enthalpy the specific humidity increases and the temperature decreases. Extent of this exchange obviously depends on the starting temperature and humidity: if already near saturation, this being the upper limit for the humidification process, there will only be a slight lowering of the temperature, whereas the temperature reduction can be really appreciable if the starting point is very dry and hot air.

Here is the strong influence of the climate on the possible advantages evaporative cooling. Starting from predefined conditions the air is humidified adiabatically ; the condition that can be achieved are limited by the saturation curve, while also considering that the saturation efficiency of the humidifier further limits the attainable values.

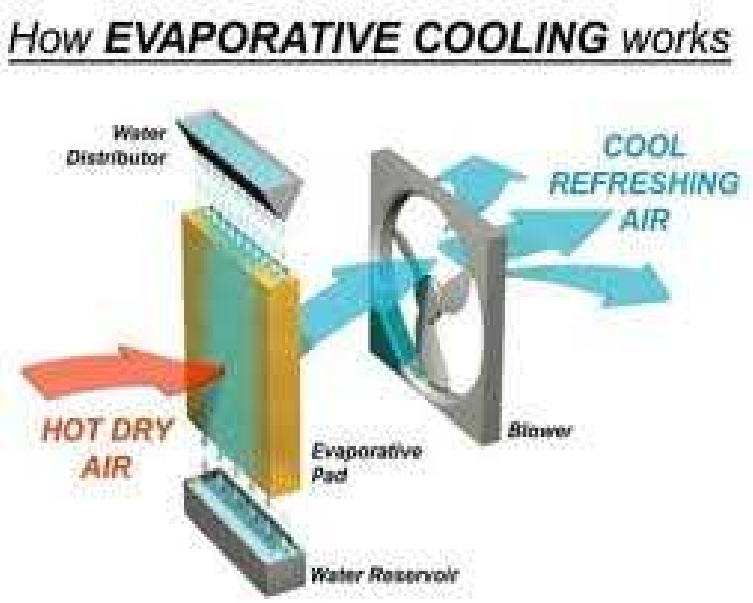


**Figure 1.4 Working of an evaporative cooler**

Evaporative cooling may be an alternative to mechanical refrigeration cooling for air conditioning depending on the climatic conditions and building load characteristics. This concept is enhanced again at the present status when energy-saving and environment-preserving are two subjects in all engineering fields due to its characteristics of zero pollution, energy efficiency, simplicity and good indoor air quality.


**Figure 1.5 Evaporative cooling pad**

The direct evaporative coolers have been used in many arid areas of the world such as south-western United States, Australia, Western Asia and north-western China. Evaporative cooling may be utilized to reduce energy consumption or to replace conventional refrigeration system

in HVAC. Different schemes of evaporative cooling and different types of equipment have been developed for such applications. Energy consumption in HVAC accounts for approximately 20% of the total energy consumption nowadays. Effective use of energy and free energy is especially important. Evaporative cooling uses free energy or recovered energy for air conditioning.

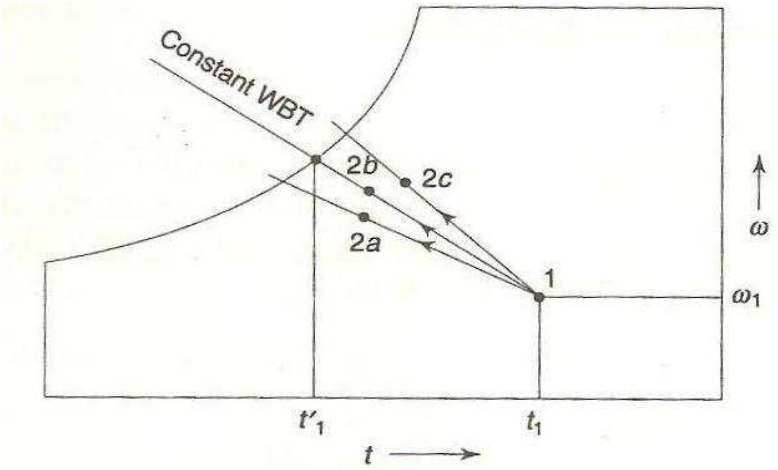


**Figure 1.6 Evaporative cooling processes on psychometric chart**

Figure 1.6 shows the evaporative cooling processes on psychometric chart. The process 1-2b corresponds to adiabatic humidification, it happens when cooling water is at wet bulb temperature of air. The process 1-2a corresponds to a lower cooling water temperature whereas 1-2c corresponds to a higher cooling water temperature.

## 1.3 Motivation of the present work

The demand of use of evaporative cooling is self explanatory. The present energy scenario and crisis of energy makes this technology a favourable one among all of the cooling technologies available However, Evaporative air cooling is an under-utilized technology worldwide that has yet to fulfil its full potential. The potential future global market and environmental benefits of this technology with increased market penetration is enormous.

Evaporative air cooling technologies alone, as well as coupled with desiccant technologies, could displace the need for vapour compression air conditioning for many applications. As Developing nations economies grow, energy saving technologies such as Evaporative air cooling will assist with future developments.

A lot of work has been done in the areas of modelling, simulation, analysis, heat and mass transfer analysis, prediction of outlet temperature, outlet humidity etc.; still there are scopes in the areas of heat and mass transfer calculations and modelling of an evaporative cooler.

Some work has been carried out in carrying out the heat and mass transfer correlations; still there is scope of developing these correlations for different inlet water temperatures, i.e. inlet water at normal, elevated and lower than Wet Bulb temperatures.

Present work carries out the effect of various parameters on performance of the evaporative cooling of air. Modelling of the system is done and experimental results are compared with the model results. Curve fitting of various data is done to establish relationship among various variables using regression analysis, both by programming and manually.

## 1.4 Organization of the report

The present work is divided into seven chapters. First chapter explains the historical background and technology behind the evaporative cooling systems. Second chapter gives details of the literature studied for present work and motivation for present work. In third chapter formulation for evaporative cooling is done on the basis of which the cooling technology is analyzed. Further the description of test rig is given in fourth chapter. The mathematical expressions developed, is given in fifth chapter. Based upon the formulation in third chapter the analysis is done in sixth chapter. The conclusions drawn from the analysis done is also discussed concluding with the future work opportunities.

# Chapter 2

# Literature Review

The study of Evaporative cooling involves several fields of engineering, namely, fluid dynamics, material science, environmental engineering, heat and mass transfer, material science and multiphase dynamics which are encountered in vast range of applications. The literature on fluid dynamics, material science, environmental engineering, heat and mass transfer, material science and multiphase dynamics is, consequently distributed across several disciplines. The literature studied for the present work can be categorized under following categories.

**2.1 Classification of literature**

2.1.1 Feasibility study

2.1.2 Classification and basis of classification

2.1.3 Applications and limitations

2.1.4 Method of analysis

2.1.5 Materials and manufacturing

## 2.1.1 Feasibility study

The evaporative-cooling systems are, by their very nature, more dependent on climatic conditions than mechanically cooled systems. Accordingly, a success achieved at one particular location cannot be offhand guaranteed or readily copied elsewhere. Feasibility of evaporative cooling should be investigated at each location individually.

**M.F.El-Refaie et al**[1] have carried out feasibility study of evaporative cooling. Their work establishes a general foundation for judging the feasibility of evaporative cooling with different evaporative-system configurations, under different climatic conditions and for different applications. Two feasibility criteria were stipulated; the rate of air supply to space

and the indoor relative humidity. Systematic procedures were presented for evaluating the required air-flow rate and predicting the achievable indoor condition. Explicit mathematical expressions were derived to define the limitations on outdoor conditions for any allowable specific air flow. The impacts of various pertinent factors were investigated. These include the required indoor temperature, the quality of space load represented by its SHF and the performance index of the system. Computer programs were devised to automate, hence facilitate, the repetitive computations and to evade the graphical work on the psychometrics chart. Samples of program results were graphically displayed.

**Yunus Cerci**[2] has discussed a new ideal evaporative freezing cycle of water in which a new ideal evaporative freezing cycle for freezing of water is proposed and analyzed by using the conservation of energy and the conservation of mass principles. The proposed cycle utilizes low temperature heat sources such as solar energy, geothermal energy, and waste heat, and consists of a freezing chamber, an air-to-air heat exchanger, a desiccant chamber, an air-to-water heat exchanger, and a fan through which air circulates at atmospheric pressure. The operating principles of the cycle is based on the fact that as dry air picks up moisture from water, the water vapor absorbs heat primarily from the remaining body of the water, and thus the water is cooled and frozen. It is shown that the proposed system can produce 28.4 g ice/kg dry air circulated at most and have a thermal coefficient of performance up to 0.47. The proposed evaporative freezing cycle offers a viable alternative to the conventional refrigeration methods and provides refrigeration by using the inexpensive source of thermal energy source. Also, various aspects of the cycle proposed are discussed.

**P. Stabat**[3] carried out a study that in low load buildings, the indirect evaporative cooling system can be sufficient to reach comfort. In high load buildings, the desiccant cooling mode can take over from indirect evaporative cooling but in very high load buildings; it turns out to be inadequate. The limits of feasibility of the indirect evaporative system and desiccant

cooling systems have been assessed by the authors. The methodology is based on simulations which have been carried out for different temperate climatic zones, different thermal inertia levels, different internal load levels and different solar gain levels. The annual energy consumption has been assessed. Since water consumption cannot be neglected when considering operating costs, it has been evaluated.

**Renato M. Lazzarin et al**[4] carried out a work on diagram based method to find out the feasibility of evaporative cooling methods for various climatic conditions and free cooling and found that direct evaporative cooling can be profitable in hot arid climates, whereas favourable situations are not frequent in temperate zones. First the climate limits to direct operation were set on the psychometric diagram. Then an alternative process was considered that can provide free cooling via evaporation for a lot of climatic conditions not particularly dry and very common in temperate climate: indirect evaporative cooling. Air was cooled in an adiabatic humidification process, and then in turn the same air is used to reduce – via a heat exchanger – the temperature of a second stream of air, whose moisture content consequently remains unchanged. The cooling effect was particularly strong when the air to be humidified is the ambient air being discharged. The potential of indirect evaporative cooling was analysed in every climatic condition, dividing the Mollier psychrometric diagram in different zones where the use of this free cooling techniques is advisable or not.

**Ghassem Heidarinejad**[5] studied that some countries have multi-climate regions, and needed to be investigated more precisely. Based on these conditions, several cooling systems can be used for each region. In their study, the potential of the direct evaporative cooling (DEC) systems, indirect evaporative cooling (IEC) systems, desiccant wheel (DW) with DEC systems, and combination of these methods for cooling in the cities of Iran were investigated. In the remaining regions, mechanical cooling systems and absorption systems can be used. According to weather condition and natural resources for water in Iran, DEC can be

considered as a serious alternative for cooling. In their paper, based on numerical simulation and long-term meteorological measurements, general set of criteria is obtained. Results show that according to population dispersal DEC systems can provide comfort conditions for 53% of people of Iran. IEC, DW, combination of these systems, and mechanical cooling systems can supply comfort condition in remaining major cities of Iran consequently. Moreover, for showing the uniqueness of weather condition which leads to these varieties of climates, other important cities in the neighbouring countries were compared with their numerical simulation code.

### 2.1.2 Classification and basis of classification

**Ren Chengqin et al**[6] have carried out exergy analysis of evaporative cooling processes classifying the evaporative cooling processes in four different groups:

1 Direct Evaporative Cooling (DEC)

2 Indirect Evaporative Cooling (IDEC)

3 Direct Indirect Evaporative Cooling (DIEC)

4 Regenerative Evaporative Cooling (REC)

The authors have suggested a functional classification to break down HVAC project in a hierarchy structure for analysis. Energy flows are also classified according to their function as source energy flow and service energy flow to assist the evaluation of the performance of the systems or components.

A quantitative work has been done by various other authors on classification of evaporative cooling processes for the purpose of analyzing the process and generally lists top three of the above listed types. Classification based upon the applicability is also done by various authors and the list involves the top three of the above listed types.

### 2.1.3 Applications and limitations:

The use of evaporative cooling system for domestic and industrial application is limited by climatic conditions. The performance is better in hot and dry climates having very low relative humidity. Generally tropical climatic conditions are the target location for the use evaporative air cooling.

**M. S. Sodha et al**[7] have carried out some work for design patterns of evaporative coolers for two different locations Jodhpur and Delhi. Studies on the effect of the relevant parameters on the cooler performance and on the effect that coolers have on the thermal performance of the building have been made. Some suitable rules of thumb for evaporative coolers have been made for common users. For floating temperature conditions, which are obtained in desert cooler coupled buildings, the thermal performance of the building may be characterized by seasonal discomfort. The study shows for the Delhi climate, which is composite climate of north India and for Jodhpur climate, which is hot dry climate, the seasonal discomfort index for a given size of room coupled with cooler decreases with fan power and pad area and packing factor of the pads of the cooler. For sizing the desert cooler for the cooling of a given floor area, the criterion is the reduction in discomfort index by 90% of its value without a cooler.

**Robert E. Foster**[8] has carried out a study on use of evaporative coolers in North America in view of greenhouse gas emissions and global warming. This study shows the benefits of using Evaporative air cooling as evaporative air cooling does not require CFC refrigerants and only requires water. Its use in place of vapour compression systems eliminates CFC and other green house emissions. Principle advantages of evaporative air cooling technologies are

1. Significant local fabrication and employment
2. Substantial energy and cost savings
3. No chlorofluorocarbon usage

4. Reduced peak power demand
5. Reduced $CO_2$ and power plant emissions
6. Improved indoor air quality
7. Life cycle cost effectiveness
8. Easily integrated into built up systems
9. Provide humidification when needed
10. Greater regional energy dependence

**Renato M. Lazzarin**[4] carried out a diagram based method for carrying out the feasibility of various evaporative cooling systems for various climatic conditions in which Systematic procedures were presented for evaluating the required air-flow rate and predicting the achievable indoor condition. Explicit mathematical equations were derived to define the limitations on outdoor conditions for any allowable specific air flow. Direct evaporative cooling can be profitable in hot arid climates, whereas favourable situations are not frequent in temperate zones. First the climate limits to direct operation are set on the psychrometric diagram. Then an alternative process is considered that can provide free cooling via evaporation for a lot of climatic conditions not particularly dry and very common in temperate climate: indirect evaporative cooling. Air is cooled in an adiabatic humidification process, and then in turn the same air is used to reduce – via a heat exchanger – the temperature of a second stream of air, whose moisture content consequently remains unchanged. The cooling effect is particularly strong when the air to be humidified is the ambient air being discharged. The potential of indirect evaporative cooling in analysed in every climatic condition, dividing the Mollier psychometric diagram in different zones where the use of this free cooling techniques is advisable or not.

**Jose Rui Camargo et al**[9] have carried out some experimental studies of direct evaporative cooler operating during summer in Brazilian city.

**Carla Fernanda Barbosa Teixeira et al**[10] have carried out a case study of Campinas, Brazil, a tropical climate, using evaporative cooling systems for human comfort.

**Ebrahim Hajidavalloo**[11] studied the use of evaporative air cooling to enhance the heat transfer rate and performance of window air conditioner. In their article, a new design with high commercialization potential for incorporating of evaporative cooling in the condenser of window-air-conditioner was introduced and experimentally investigated. A real air conditioner was used to test the innovation by putting two cooling pads in both sides of the air conditioner and injecting water on them in order to cool down the air before it passing over the condenser. The experimental results showed that thermodynamic characteristics of new system are considerably improved and power consumption decreases by about 16% and the coefficient of performance increases by about 55%.

**Marcos B bellorio**[12] studied the use of evaporative cooling on gas turbine. A mathematical model for both evaporative cooling and gas turbine based on mass and energy balance was developed and results show that use of evaporative cooling increased the power output and decreased NOx emissions.

**João M. D. Pimenta et al**[13] carried out an engineering study concerning the application of evaporative cooling systems for small-scale power generation and ambient thermal comfort is presented in their paper. A first case study considered an analysis on the potential of a direct evaporative media coupled to an existing gas micro turbine cycle. The layout of the thermal system in study, with air combustion evaporative cooling of the cycle, was presented. The mathematical model adopted for computational simulation was based in classical principles of mass and energy conservation, for the thermodynamics processes involved. A parametric study of the effects of the air combustion evaporative cooling about variables as cycle efficiency and output power, was investigated, so the micro turbine performance along the test reference year (TRY) in Brasilia. The second case study is related to the application of an

evaporative cooling system for space conditioning of the Community Centre of the University of Brasilia. Initially, constructive, occupation and orientation aspects were characterized. Next a methodology for cooling load hourly calculation is presented based in an energy balance applied for each individual element of the canvas elliptic surface peculiar geometry treated by a rendering numeric process. The determination of the evaporative cooling system was realized based in the maxim thermal load calculated for a Test Reference Year in Brasilia. The evaporative cooling system simulation consisted in the response of dry bulb temperature and relative humidity within building during the analysis time. Results obtained for the first case showed that a direct evaporative system can increase power output and decreases specific fuel consumption in a micro turbine based power generation cycle. For the second case, it was verified that an evaporative cooling system use for thermal comfort in the community centre is recommendable in that year periods when dry bulb temperature and relative humidity outside building are higher than internal comfort conditions.

**M. Maerefat et al**[14] in their study proposed a system consisting of a Solar Chimney (SC) and an Evaporative Cooling Cavity (ECC) to enhance passive cooling and natural ventilation in a solar house. The capability of the system to meet the required thermal needs of individuals and the effects of main geometric parameters on the system performance had been studied. The dependence of the system performance on outdoor air temperature has been studied to determine the operative conditions for appropriate effectiveness, regarding thermal comfort criteria. To determine the heat and mass transfer characteristics of the system, a mathematical model based on conservation equations of mass and energy had been developed and solved by an iterative method. The findings show that the system is capable of providing good indoor air condition at daytime in a living room, even with poor solar intensity of 200 W/m2. The results show that when the relative humidity is lower than 50%, the system can make good indoor air condition even at $40^0$C, and a higher performance is achieved using ECC

with concurrent configuration. It is found that the proposed system may be applied successfully in hot arid climates to fulfil the indoor thermal comfort expectations.

**Ebrahim Hajidavalloo et al**[15] in their study proposed a new design with high commercialization potential for incorporating of evaporative cooling in the condenser of window-air-conditioner is introduced and experimentally investigated. A real air conditioner was used to test the innovation by putting two cooling pads in both sides of the air conditioner and injecting water on them in order to cool down the air before it passing over the condenser. The experimental results show that thermodynamic characteristics of new system are considerably improved and power consumption decreased by about 16% and the coefficient of performance increased by about 55%.

**Khalid A. Joudi et al**[16] conducted into the application of the indirect evaporative cooling in fulfilment of the variable cooling load of a typical Iraqi dwelling. A two story house located in Baghdad was the object of the study. The application was evaluated through a systematic simulation, along with a comparison between two arrangements of an indirect-direct evaporative cooling system. The simulation involved the operation of the cooling system under four operating modes for variable ambient temperature and cooling load conditions during the summer season. The concept of variable air volume (VAV) was employed as a control strategy over the day by changing the supply air low rate through a variable speed fan according to the variation in the cooling load. Hourly computerized calculations were programmed for the variable cooling load using the transfer function method (TFM) over 24 hour daily cycles. The simulation of the system included variation in the effectiveness of the plate heat exchanger employed for the indirect evaporative cooling stage and its effect upon the variation in the air low rate. The results showed that indirect evaporative cooling would result in a comfortable indoor condition for most periods of system operation. Also, the

results have shown that the coefficient of performance tends to be very high because the system consumes only fan and water pumping power.

**Charles Kutscher et al**[17] described a spreadsheet model that was developed to assess the cost and performance of four methods for using supplemental evaporative cooling to boost summer performance of geothermal power plants: 1) pre-cooling with spray nozzles, 2) pre-cooling with Munters media, 3) a hybrid combination of nozzles and Munters media, and 4) direct deluge cooling of the air-cooled condenser tubes. Although all four options show significant benefit, deluge cooling has the potential to be the most economic.

**E.E. Anyanwu**[18] proposed a porous media evaporative cooler for preservation of fruits and vegetables. The experimental cooler, with a total storage space of 0.014 $m^3$, consisting of a cuboids shaped porous clay container located inside another clay container. The gap between them was filled with coconut fibre. A water reservoir linked to the cooler at the top through a flexible pipe supplied water to fill the gap, thus keeping the coconut fibre continuously wet. Results of the transient performance tests revealed that the cooler storage chamber temperature depression from ambient air temperature varied over 0.1–12$^0$C. Ambient air temperatures during the test periods ranged over 22–38$^0$C. The results also illustrate superior performance of the cooler over open air preservation of vegetables soon after harvest during the diurnal operations. Thus, the evaporative cooler has prospects for use for short term preservation of vegetables and fruits soon after harvest.

## 2.1.4 Method of analysis

Energy consumed in HVAC accounts for approximately 20% of total energy consumption now a day. Effective use of energy and free energy is especially important. Evaporative cooling may be utilized to reduce energy consumption or to replace conventional refrigeration system in HVAC, as it uses free energy or recovered energy. The second law of

thermodynamics tells us that the maximum available energy of moist air that may be recovered or utilized is its exergy. Therefore, the energy saving potential ought to be exergy. This potential is independent of schemes and equipments to be used and will be useful for comparison of the performances. The exergy method calculates the exergy loss caused by irreversibility, which is an important thermodynamic property, which measures the useful work that can be produced by a substance. Analysis of exergy losses provides information as to where the real inefficiencies in a system lie.

**Kunxiong Tan et al**[19] have carried out a numerical analysis of reversibly used water cooling towers in which they have applied a desuperheater heat recovery system for service hot-water heating for subtropical regions. However, in colder seasons when building cooling load is reduced, a standard water-cooling tower may be reversibly used to extract free heat from ambient air to make up the reduction of heat source for water heating. Previous related work included developing an analytical method for evaluating the heat and mass transfer characteristics in a reversibly used water-cooling tower (RUWCT), which cannot be used to determine the air and water states at any intermediate horizontal sections along the tower height within an RUWCT. This paper presents a detailed numerical analysis by which the air and water states at any horizontal plane along the tower height within an RUWCT can be determined. The numerical analysis has been partially validated using the experimental data from an installed RUWCT in a hotel building in southern China. The numerical analysis reported in this paper, together with the Analytical Method previously developed, provides a complete method for the analysis of heat and mass transfer characteristics within and at the boundaries of an RUWCT.

**Taufiq B.N. et al**[20] have carried out a study about energy efficiency of evaporative cooling systems over conventional refrigeration systems. The study also focuses about environmental impacts of evaporative cooling systems.

**Chengqin Ren et al**[21] have carried out the exergy analysis of evaporative cooling systems. In the study an unusual dead state, other than atmospheric state is selected for exact analysis. Various types of evaporative cooling systems are compared. Concluded with that II law efficiency is the right measure to analyze the evaporative cooling systems

**Wu J.M. et al**[22] concludes that the frontal air velocity and pad thickness of the pad module are two key influencing factors to the cooling efficiency of a direct evaporative cooler. The optimum frontal velocity of the pad module should be around 2.5 m/s for the needed supply volume. This recommended value can be used to decide the frontal area of the pad modules in a direct evaporative cooler. Too small a velocity will result in a large frontal area of the pad module and an increase in size and primary investment of direct evaporative cooler.

In the **numerical investigation**[23] the authors developed a set of simplified governing equations to describe heat and moisture transfer between water and air in the evaporative cooler. The influences of the inlet frontal air velocity, pad thickness, inlet air dry bulb temperature and wet bulb temperature on the cooling efficiency of the evaporative cooler are analyzed in the same paper.

**Ala Hasan**[24] suggested a method to cool the air below its wet bulb temperature. The ultimate temperature for such a process is the dew point temperature of the ambient air. The author concludes that the cooling effect obtained by any indirect evaporative coolers is dependent on both the temperature and flow rate of the delivered product air to the room. For a specified total inlet air flow rate for a cooler, increasing the working air flow rate results in a lower temperature, and lower flow rate, for the delivered product air and vice-versa. This is then an optimization problem where objective is to maximize the cooling power to the delivered product air.

**Ghassem Heidarinejad et al**[5] show that considering the climatic conditions variety of, the two stage direct/indirect has high potential to provide comfort conditions in regions where at

present stand-alone direct evaporative coolers cannot provide comfort conditions. Also in regions with high wet bulb temperatures, this system can be used instead of mechanical vapour compressions systems, so leading to decrease in electrical energy consumption. Results show that average water consumption of two-stage evaporative cooling system is 55% more than direct evaporative cooling system and power consumption is 33% of mechanical vapour compression system, so this cooling system can be used in various climatic conditions as an environmentally clean and energy efficient system.

**Dowdy J.A.**[25] in performance of a rigid cellulose evaporative medium for elevated inlet water temperatures has obtained temperature correlations to predict the performance of a rigid impregnated cellulose evaporative medium with inlet water temperatures between those of ambient dry bulb temperature and wet bulb temperature. His study considers mass flow rate ratios of water to air up to 0.8 in value.

**B. Riangvilaikul et al**[26] analyzed a novel dew point evaporative cooling system for sensible cooling of ventilation air. Investigation on the outlet air conditions and the system effectiveness at different inlet air conditions (temperature, humidity and velocity) covering dry, temperate and humid climates. The results showed that wet bulb effectiveness ranged between 92 and 114% and the dew point effectiveness between 58 and 84%. A continuous operation of the system during a typical day of summer season in a hot and humid climate showed thatwet bulb and dew point effectiveness were almost constant at about 102 and 76%, respectively.

**R. Sureshkumar et al**[27] generated experimental data on evaporative cooling. Heat and mass transfer processes between a water spray and ambient air. Four nozzle sizes were tested for hot-dry and hot-humid conditions that covered DBT from 35 to 47 $^{0}$C, and R.H. 10–60% in parallel and counter flow configurations. Three water pressures 1, 2 and 3 bar(g) and three air velocities 1, 2 and 3 m s_1 completed the test matrix. A simulation model for two-way

coupling of heat and mass transfer between the droplets and air is described here. Using the Maximum Entropy Formulation, droplet diameter–velocity combinations were generated and classified into 200 parcels that were the initial conditions for droplet motion. Simulation results and experimental data agree within ±15% for parallel and ±30% for counter flow configurations.

**Renato M. Lazzarin et al**[4] proposed a diagram based method to evaluate the evaporative cooling technology, which also supplies information about the feasibility as per the ambient conditions available.

**A.S. Kaiser et al**[28] developed a numerical model for studying the evaporative cooling processes that take place in a new type of cooling tower. In contrast to conventional cooling towers, this new device called Hydro solar Roof presents lower droplet fall and uses renewable energy instead of fans to generate the air mass flow within the tower. The numerical model developed to analyse its performance is based on computational flow dynamics for the two-phase flow of humid air and water droplets. The Eulerian approach is used for the gas flow phase and the Lagrangian approach for the water droplet flow phase, with two-way coupling between both phases. Experimental results from a full-scale prototype in real conditions have been used for validation. The main results of this study show the strong influence of the average water drop size on efficiency of the system and reveal the effect of other variables like wet bulb temperature, water mass flow to air mass flow ratio and temperature gap between water inlet temperature and wet bulb temperature. Non dimensional numerical correlation of efficiency as a function of these significant parameters has been calculated.

**Y.J. Dai et al**[29] analyzed cross-flow direct evaporative cooler, in which the wet durable honeycomb paper constitutes as the packing material. The system is expected to act as both humidifier and evaporative cooler to create a comfortable indoor environment in arid regions.

A mathematical model, including the governing equations of liquid film and gas phases as well as the interface conditions, has been developed. The interface temperature of falling film has been predicted and discussed in detail. Analysis results indicate that there exists an optimum length of the air channel, which results in the lowest temperature, and the system performance can be further improved by optimizing the operation parameters, such as the mass flow rates of feed water and process air, as well as the different dimensions of the honeycomb paper.

**Chung-Min Liao et al**[30] developed a compact wind tunnel to simulate evaporative cooling pad–fan systems and to provide direct measurement of system performance. Two alternative materials including one made of coarse fabric PVC sponge mesh 2.5 mm diameter in pinhole and one made of 6ne fabric PVC sponge mesh in 7.5 mm diameter pinhole were tested as pads in wind tunnel experiment. Authors have experimentally examined the effects of air velocity, water flow rate, static pressure drop across pad, and pad thickness on evaporative cooling efficiency. Pad face velocities and associated static pressure drops that allow a pad–fan system works were measured. The dimensionless working equations of heat and mass transfer coefficients through various thicknesses of alternative pad media could be obtained through curve fitting technique based on the measurements.

**Boris Halasz**[31] developed a general non dimensional mathematical model for the description of all types of evaporative cooling devices in today's use (water cooling towers, evaporative condensers and evaporative fluid coolers, air washers, dehumidifying coils etc.). The system of differential equations describing non-adiabatic evaporation processes is transformed to a pure non dimensional form by the introduction of non dimensional coordinates and parameters and by the substitution of a straight air saturation line instead of the real one. In such a way, not only the description of the entire process becomes very simple, but also the overall performance of any such device can be expressed in terms of only few parameters and

presented in one or few diagrams. This non dimensional model forms a basis for simple and rather accurate methods for rating various types of evaporative cooling devices. For every type of device, a unique rating procedure can be established, irrespective of the relative flow direction of the fluids involved, which is very convenient when cross-flow devices are considered. Since every particular type of evaporative device deserves considerable attention, the application of this general model to various evaporative devices, together with the resulting rating procedure and accuracy test will be presented in detail in the follow-on papers, each devoted to one particular type.

**Qun Chen et al**[32] extended the entransy theory using the analogy between heat and mass transfer processes to tackle the coupled heat and mass transfer processes so as to analyze and optimize the performance of evaporative cooling systems. Introducing a few new concepts including the moisture entransy, moisture entransy dissipation, and the thermal resistance in terms of the moisture entransy dissipation. Thereinafter, the moisture entransy is employed to describe the endothermic ability of a moist air. The moisture entransy dissipation on the other hand is used to measure the loss of the endothermic ability, i.e. the irreversibility, in the coupled heat and mass transfer processes e this total loss is shown to consist of three parts: (1) the sensible heat entransy dissipation, (2) the latent heat entransy dissipation, and (3) the entransy dissipation induced by a temperature potential. Finally the new thermal resistance, defined as the moisture entransy dissipation rate divided by the squared refrigerating effect output rate, is recommended as an index to effectively reflect the performance of the evaporative cooling system. In the end, two typical evaporative cooling processes are analyzed to illustrate the applications of the proposed concepts.

**A. Fouda et al**[33] developed a mathematical model to describe the heat and mass transfer between air and water in a direct evaporative cooler. The model consists of the governing equations with their boundary conditions and some associated algebraic equations. The

related latent heat of water evaporation is taken as a heat source in the energy equation, and the mass of evaporated water is treated as a mass source in the mass equation. The study presents a comparison of the computed results with that of experimental results for the same evaporative cooler. A good agreement between the calculated and experimental results is achieved. The influences of the inlet frontal air velocity, pad thickness, inlet air dry-bulb temperature on the cooling efficiency of the evaporative cooler are calculated and analyzed. The predicted results show validity of simple mathematical model to design the direct evaporative cooler, and that the direct evaporative cooler with high performance pad material may be well applied for air conditioning systems.

**M. Lemouari et al**[34] carried out experimental analysis of simultaneous heat and mass transfer phenomena between water and air by direct contact in a packed cooling tower. The tower is filled with a ‘‘VGA.” (Vertical Grid Apparatus) type packing. The packing is 0.42 m high and consists of four (04) galvanised sheets having a zigzag form, between which are disposed three (03) metallic vertical grids in parallel with a cross-sectional test area of 0.15 m -0.148 m. This study investigates the effect of the air and water flow rates on the global heat and mass transfer coefficient as well as the evaporation rate of water into the air stream, for different inlet water temperatures. Two operating regimes were observed during the air/water contact inside the tower, a Pellicular Regime (PR) and a Bubble and Dispersion Regime (BDR). These two regimes can determine the best way to promote the heat and mass transfer phenomena in such device

**R. Sureshkumar et al**[35] presented experimental data obtained for two ambient conditions, viz., hot-dry and hot-humid, covering dry bulb temperature (DBT) from 35 to 47 $^{0}$C, and R.H. 10–60%. The studies were conducted for parallel and counter flow configurations, each with four nozzle sizes; water pressures were 1, 2 and 3 bar(g) and air velocities 1, 2 and 3 m/s. The controls on air and water conditions, and the accuracy of measurement were improved so that the uncertainties are considerably lower than in earlier studies. The data

showed clear trends. For a specific water flow rate, a smaller nozzle at higher pressure produced more cooling than a larger nozzle at lower pressure.

**B. Costelloe et al[36]** examined the performance of an open industrial scale cooling tower, utilising small approach temperature differences (1–3 K), for rejection of heat at the low water temperatures (11–20$^0$C) typical of chilled ceilings and other sensible air–water heat dissipation systems in buildings. The study was carried out under temperate maritime climatic conditions (3–18$^0$C wet-bulb temperature range). Initially a theoretical analysis of the process at typical conditions for this climate was conducted, which indicated that a water to air (L/G) mass flow rate ratio of less than 1.0 was required for effective operation. Consequently for these low L/G ratios, the thermal performance of the experimental tower was measured and correlated. A new correlation is proposed which shows a significant increase in the NTU level achieved, for the required L/G ratios (0.3–0.9). As the cooling tower in this application is predominantly a mass transfer device under summer conditions, the evaluation of the total volumetric heat and mass transfer coefficient is of particular relevance and is also determined.

**A. Beshkani et al[37]** mathematically modelled and evaluated the performance of rigid media evaporative cooler, equipped with corrugated papers as a wetted medium. The governing equations of air were solved using finite difference analysis and Projection algorithm. Saturation efficiency and pressure drop as functions of air velocity and media depth were calculated. Effects of corrugation shape, mean plate space, Reynolds number and Prandtl number were also considered. Analysis of the results showed that efficiency improves with decreasing velocity and increasing depth of media. Pressure drop increases with increase of both velocity and media depth. In addition, efficiency becomes approximately independent of velocity with increasing depth to a certain value. Results obtained were compared with those of channel flow and showed that, corrugating one side of the channel at high velocity can improve efficiency by 40%.

**Paisarn Naphon**[38] investigated both experimental and theoretical results of the heat transfer characteristics of the cooling tower. A column packing unit was fabricated from the laminated plastic plates consists of eight layers. Air and water were used as working fluids and the test runs were done at the air and water mass flow rates ranging between 0.01 and 0.07 kg/s and between 0.04 and 0.08 kg/s, respectively. The inlet air and inlet water temperatures are $23^0$C, and between 30 and $40^0$C, respectively. A mathematical model based on the conservation equations of mass and energy was developed and solved by an iterative method to determine the heat transfer characteristics of the cooling tower. There is reasonable agreement from the comparison between the measured data and predicted results.

**Hakan Caliskan et al**[39] presented energy and exergy analysis and sustainability assessment of the novel evaporative air cooling system based on Maisotsenko cycle which allows the product fluid to be cooled in to a dew point temperature of the incoming air. In the energy analysis, Maisotsenko cycle's wet-bulb and dew point effectiveness, COP and primary energy ratio rates are calculated. Exergy analysis of the system is then carried out for six reference temperatures ranging from $0^0$C to $23.88^0$C as the incoming air (surrounding) temperature. The specific flow exergy, exergy input, exergy output, exergy destruction, exergy loss, exergy efficiency, exergetic COP, primary exergy ratio and entropy generation rates are determined for various cases. Furthermore, sustainability assessment is obtained using sustainability index method. As a result, maximum exergy efficiency is found to be 19.14% for a reference temperature of $23.88^0$C where the optimum operation takes place.

**B.N. Taufiq et al**[40] described the modelling and optimization analysis for cooling system in the building. Exergy technique has been used to evaluate overall and component efficiencies and to identify thermodynamic losses. The method is well suited for analyzing thermodynamic model and identified exergy losses of air conditioning application in a building.

**Ren Chengqin et al**[41] discussed the principles of exergy analysis in heating ventilating and air conditioning (HVAC through an analytical review of some pertinent works. An unusual selection of dead-state novel to HVAC applications is suggested, which simplifies the exergy analysis by eliminating the necessity of calculating the exergy of water at ambient temperature.

### 2.1.5 Materials and manufacturing

Evaporative air cooling unit is essentially a relatively simple technology that can wholly or partially produced in less developed countries, depending on the existing industrial base. In India and Pakistan for instance large Volumes of complete units are being produced locally. Small enterprises use a labour intensive production process in India. The products are made of sheet metal, wood fibre pads and simple pump, finding their way on the market either as finished products or as kits, transported all over the India. The other type of fabrication are more sophisticated indirect-direct evaporative cooler production in Australia and the USA, with coated sheet metal, plastics or fibre glass, efficient cellulose paper-pads, computerized thermostats and bleed-offs. These units are marketed with glossy folders and exported to a number of countries.

**Dai Y.J. et al**[29] discussed about honeycomb paper as packing material in evaporative coolers, and concludes that the evaporative cooler using honeycomb paper as packing materials is compact in size and weights less; it can as well act as a humidifier in arid region. Under typical conditions it can reduce the air temperature by $9^0$C and increase the humidity ratio by about 50%.

**Chung-Min Liao et al**[30] discusses about various alternative cooling pad materials available locally and their feasibility.

## 2.2 Conclusions of literature review

A lot of work has been done on the feasibility studies, materials, performance analysis of evaporative cooling systems and heat and mass transfer analysis. The counted research gap may be the heat and mass transfer correlations for different inlet water temperatures. **Dowdy J.A.**[25] has established these correlations for normal inlet water temperatures. Hence there is scope of developing correlations for different inlet water temperatures.

## 2.3 Objectives of present work

A lot of work has been done in the areas of modelling, simulation, analysis, heat and mass transfer analysis, prediction of outlet temperature, outlet humidity etc.; still there are scopes in the areas of heat and mass transfer calculations and modelling of an evaporative cooler. Some work has been carried out in carrying out the heat and mass transfer correlations; still there is scope of developing these correlations for different inlet water temperatures, i.e. inlet water at normal, elevated and lower than Wet Bulb temperatures. Present work carries out the effect of various parameters on performance of the evaporative cooling of air. Modelling of the system is done and experimental results are compared with the model results. Curve fitting of various data is done to establish relationship among various variables using regression analysis, both by programming and manually. Correlations for heat and mass transfer are established in form of various dimensionless numbers.

# Chapter 3

# Formulations of evaporative cooling systems

Evaporative cooling occurs when moisture is added to air that has a relative humidity of less than 100 percent. The lower the relative humidity, the greater the temperature drops when moisture is added. Their key process is heat and moisture transfer between air and water. The use of evaporation of water in air conditioning is an old and much known technology. However its importance is again being recognized due to characteristics of zero pollution, energy efficiency, simplicity and good indoor air quality. The principle of evaporative cooling indicates that the evaporative cooling system can only remove sensible heat, thus the evaporative cooling system works best in hot and dry climate where the maximum evaporative cooling will result. All humidification systems that use liquid involve an exchange between the latent heat and the sensible heat in the air stream: the latent heat portion increases, the sensible portion decreases. For an essentially unvaried enthalpy the specific humidity increases and the temperature decreases. Extent of this exchange obviously depends on the starting temperature and humidity: if already near saturation, this being the upper limit for the humidification process, there will only be a slight lowering of the temperature, whereas the temperature reduction can be really appreciable if the starting point is very dry and hot air.

The formulation of evaporative cooling process need to be done for both model and experimental values for:

(i) Basic relationship between dimensionless numbers for force convection heat transfer

(ii) Heat transfer coefficient

(iii) Mass transfer coefficient

(iv) Relationship between heat and mass transfer coefficients

(v) Outlet air dry bulb temperature

(vi) Outlet air specific humidity

(vii) Cooling efficiency

(viii) Exergy analysis

(ix) Regression analysis for curve fitting and correlations between various parameters

## 3.1 The relationship between non dimensional numbers for heat and mass transfer for force Convection heat transfer:

Force convection heat transfer depends upon the below given variables

μ= *Kinematic viscosity of flowing air*

$\rho = Density$

$V = Velocity\ of\ flow$

$h_c = Heat\ transfer\ coefficient$

$d = Characteristic\ dimension$

$k = Thermal\ conductivity$

$c_p = specific\ heat$

Hence any of these can be written as function of others, i.e.

$h_c = f(\mu, \rho, V, d, c_p, k)$

Hence these can be set in non dimensional groups using Buckingham π Theorem,

Dimensions of all the variables

$\rho = ML^{-3}$; $V = LT^{-1}$; $d = L$; $\mu = ML^{-1}T^{-1}$; $c_p = L^2T^{-2}\theta^{-1}$

$k = MLT^{-3}\theta^{-1}$; $h_c = MT^{-3}\theta^{-1}$

Here, number of fundamental dimensions (m) = 4

Number of independent variables (n) = 7

Hence number of π terms = n-m=7-4=3

Hence this group of variables can be arranged in three non dimensional groups, i.e. 3 π terms.

$$\pi_1 = \left[ (\rho)^a \ (d)^b \ (\mu)^c \ (c_p)^d \ V \right]$$

$$\pi_2 = \left[ (\rho)^a \ (d)^b \ (\mu)^c \ (c_p)^d \ k \right]$$

$$\pi_3 = \left[ (\rho)^a \ (d)^b \ (\mu)^c \ (c_p)^d \ h_c \right]$$

Arranging for dimensions for all the variables we get three non dimensional numbers:

$$Nusselt\ number = N_u = \left(\frac{h_c d}{k}\right)$$

$$Reynold's\ number = R_e = \left(\frac{\rho V d}{\mu}\right)$$

$$Prandtl\ number = Pr = \left(\frac{\mu c_p}{k}\right)$$

This could be arranged as

$$\boldsymbol{N_u = C(R_e)^a(Pr)^b} \qquad (\mathbf{3.1})$$

Similarly for convective mass transfer the arrangement of non dimensional numbers are

$$\boldsymbol{Sh = C(R_e)^a(Sc)^b} \qquad (\mathbf{3.2})$$

Where

$$Sherwood\ number(Sh) = \left(\frac{h_m l}{k}\right)$$

$$Schmid\ number(Sc) = \left(\frac{\mu}{\rho d}\right)$$

### 3.2 Theoretical Heat transfer coefficient:

Dowdy [25] has presented correlation for heat transfer coefficient in evaporative cooling systems for rigid evaporative cellulose media:

$$Nu = 0.1(l_e/l)^{0.12} Re^{0.8} Pr^{\frac{1}{3}} \quad (3.3)$$

$l_e = 0.00285\ m\ for\ rigid\ cellulose\ medium$

$l = length\ of\ one\ pass\ of\ pad\ module, which\ is$

$l = 0.1 \div cos45° = 0.1414\ m\ \ for\ a\ thickness\ of\ 0.1m\ of\ pad\ module$

$as\ angle\ of\ pass\ of\ honeycomb\ chamber\ is\ 45°$

$$Nu = 0.1(0.00285/0.1414)^{0.12} Re^{0.8} Pr^{\frac{1}{3}}$$

$$Nu = 0.0652\ Re^{0.8} Pr^{\frac{1}{3}}$$

$$\left(\frac{h_c l}{k}\right) = 0.0652\ \left(\frac{Vl}{\nu}\right)^{0.8} \left(\frac{\mu C_{pma}}{k}\right)^{\frac{1}{3}} \quad (3.4)$$

### 3.3 Similarly for mass transfer coefficient, the correlation presented by dowdy [25], is

$$Sh = 0.08(l_e/l)^{0.12} Re^{0.8} Sc^{\frac{1}{3}} \quad (3.5)$$

$$Sh = 0.08(0.00285/0.1414)^{0.12} Re^{0.8} Sc^{\frac{1}{3}}$$

$$Sh = 0.0522\ Re^{0.8} Sc^{\frac{1}{3}}$$

$$\frac{h_m l}{d} = 0.0522 \left(\frac{\rho v l}{\mu}\right)^{0.8} \left(\frac{\mu}{\rho d}\right)^{\left(\frac{1}{3}\right)} \quad (3.6)$$

The properties of air used in above equations are at mean temperature i.e. algebraic mean of inlet and outlet air temperatures.

For a particular arrangement, if there is not much variation of mean temperature the heat and mass transfer coefficients for different flow velocities can be presented in form of velocity of air flow only, as all other things will remain constant.

## 3.4 Practical heat and mass transfer coefficients:

To find out practical heat and mass transfer coefficients the convective heat transfer equation (Newton's law of heating and cooling) can be used:

$$q = h_c A_s \Delta T \quad (3.7)$$

Where $\Delta T$ is logarithmic mean temperature difference, given as

$$\Delta T = \frac{(T_{out} - T_{in})}{\ln \frac{(T_{out} - T_{wb})}{(T_{in} - T_{wb})}} \quad (3.8)$$

And q is convective heat transferred, given as

$$q = \left(m_{a,in} C_{pma} T_{in} - m_{a,out} C_{pma} T_{out}\right) + w_{in}(m_{a,in} h_{w,in} - m_{a,out} h_{w,out})$$

$$-w_{out}(m_{a,in} h_{w,out} - m_{a,out} h_{w,wb}) \quad (3.9)$$

To find mass transfer coefficient, the convective mass transfer equation can be used, given as

$$m_e = h_m A_s \Delta \rho_v \quad (3.10)$$

Where $m_e$is water evaporation rate, and $\Delta\rho_v$ is logarithmic mean density difference of flowing air, given as

$$m_e = m_{a,out}w_{out} - m_{a,in}w_{in} \tag{3.11}$$

$$\Delta\rho_v = \frac{(\rho_{v,out} - \rho_{v,in})}{\ln\frac{(\rho_{v,out}-\rho_{wb})}{(\rho_{v,in}-\rho_{wb})}} \tag{3.12}$$

From the above two relations the practical heat and mass transfer coefficients can be evaluated and compared with the theoretical values.

### 3.5 Relationship between heat and mass transfer coefficients:

Based on assumption of $L_e = 1$,

$$\frac{h_c}{h_m} = c_{pma} \tag{3.13}$$

### 3.6 Outlet Temperature:

Outlet temperature of air can be found out using energy balance for air,

$$h_c dA_s(t_s - t) = m_a c_{pma} dt \tag{3.14}$$

$$h_c dA = m_a c_{pma}\left(\frac{dt}{(t_s - t)}\right) \tag{3.15}$$

Integrating

$$h_c A_s = -m_a c_{pma} ln(t_s - t) + C \tag{3.16}$$

Applying boundary conditions

At x=0, $t=t_1$, A=0

Hence

$$C = m_a c_{pma} ln(t_s - t_1) \tag{3.17}$$

Substituting for C in (3.3)

$$h_c A_s = -m_a c_{pma} ln(t_s - t) + m_a c_{pma} ln(t_s - t_1) \tag{3.18}$$

$$\frac{h_c A_s}{m_a c_{pma}} = ln \frac{(t_1 - t_s)}{(t - t_s)} \tag{3.19}$$

$$h_c = \frac{m_a c_{pma}}{A_s} \ln \left[ \frac{t_1 - t_s}{t - t_s} \right] \tag{3.20}$$

Assuming ideal process, the outlet temperature may be written as

$$t_{out} = t_{wb} + \left(t_{in} - t_{wf}\right) \exp\left( - \frac{h_c A_s}{m_a c_{pma}} \right) \tag{3.21}$$

**Also, conservation of energy can be used to find out the outlet temperature, as**

$$Energy\ going\ in = Energy\ going\ out$$

$$m_{a,in} \times h_{a,in} + m_{w,in} \times h_{w,in} = m_{a,out} \times h_{a,out} + m_{w,out} \times h_{w,out} \tag{3.22}$$

## 3.7 Outlet humidity:

$$w_{out} = w_s - \frac{c_{pma}}{h_{fg}} (t_{in} - t_{wb}) \exp\left( - \frac{h_c A_s}{m_a c_{pma}} \right) \tag{3.23}$$

## 3.8 Cooling Efficiency:

$$\eta = \frac{(t_{in} - t_o)}{(t_{in} - t_{wb})} \tag{3.24}$$

OR

$$\eta = 1 - \frac{(t_o - t_{wb})}{(t_{in} - t_{wb})} \tag{3.25}$$

OR

$$\eta = 1 - \exp\left(\frac{h_c A_s}{m_a c_{pma}}\right) \tag{3.26}$$

### 3.9 Humidifying efficiency

$$\eta_h = \frac{(w_{out} - w_{in})}{(w_s - w_{in})} \tag{3.27}$$

### 3.10 Energy balance at cooling pad:

$$m_{a,in}h_{a,in} + m_{w,in}h_{w,in} = m_{a,out}h_{a,out+}m_{w,out}h_{w,out} \tag{3.28}$$

OR

$$m_{da}dh_a = -[m_{w,in} - m_{da}(w_{out} - w)]h_{f,w+}m_{da}dwh_{f,w} \tag{3.29}$$

### 3.11 Exergy analysis:

Exergy analysis can be used as a reliable tool for analyzing energy consumption of any thermodynamic system or unit. Exergy analysis of evaporative cooling schemes is discussed through an analytical review of some pertinent works. For evaluation of evaporative cooling, the exergy of moist air is analyzed and broken down into three components: Thermal, Mechanical and Chemical exergy. Evaporative cooling processes are analyzed with the help of devised diagrams which are applicable to various conditions and ambient states among various cooling applications. Different cooling schemes are properly evaluated and compared in terms of exergetic efficiency. Further, to eliminate the necessity of calculating the exergy of water at ambient temperature, a dead state novel to evaporative cooling schemes is suggested, which will also make it easier to evaluate the theoretical limit of evaporative cooling capacity. The method is well suited for analyzing thermodynamic model and identifying exergy losses of air conditioning applications.

**The exergy of moist air is given by [43] (derived from entropy principle):**

$$ex = (Cpa + wCpv)\left[T - T_0 - T_0 ln\left(\frac{T}{T_0}\right)\right] + (1 + 1.608w)RaT_0 ln\left(\frac{p}{p_0}\right)$$
$$+ RaT_0\left\{(1 + 1.608w)ln\left[\frac{1 + 1.608w_0}{1 + 1.608w}\right] + 1.608wln\left(\frac{w}{w_0}\right)\right\} \quad (3.30)$$

**This may be broken down into three components, viz.**

### 3.11.1 Thermal Exergy

$$exth = (Cpa + wCpv)\left[T - T_0 - T_0 ln\left(\frac{T}{T_0}\right)\right] \quad (3.31)$$

### 3.11.2 Mechanical Exergy

$$exme = (1 + 1.608w)RaT_0 ln\left(\frac{p}{p_0}\right) \quad (3.32)$$

### 3.11.3 Chemical Exergy

$$exch = RaT_0\left\{(1 + 1.608w)ln\left[\frac{1 + 1.608w_0}{1 + 1.608w}\right] + 1.608wln\left(\frac{w}{w^0}\right)\right\} \quad (3.33)$$

Such that the total exergy is sum of the three components,

$$ex = exth + exme + exch \quad (3.34)$$

The exergy destruction in various processes with different inlet water temperatures needs to be evaluated.

### 3.11.4 Exergy destruction:

$$Exergy\ destructed = (exth + exme + exch)_{in} - (exth + exme + exch)_{out} \quad (3.35)$$

The thermal and mechanical exergies are zero for environmental air if the reference stage is environmental stage. Chemical and thermal exergy need to be evaluated at inlet and outlet conditions of air. Hence, exergy destructed

$$Exergy\ destructed = (exch)_{in} - (exch + exth)_{out} \quad (3.36)$$

### 3.11.5 Exergetic efficiency:

$$\eta_{exergetic} = \left(\frac{Exergy\ at\ outlet}{Exergy\ at\ inlet}\right) \quad (3.37)$$

## 3.12 Regression analysis for curve fitting and development of correlations between various parameters [42]:

The procedure of obtaining a best fit to a given data set is often known as regression. The regression may be

(a) Linear

(b) Polynomial

(c) Exponential/power law

**Procedure:**

$$f(x) = C_0 + C_1x + C_2x^2 + C_3x^3 + \ \ldots\ldots\ldots\ldots\ldots + C_mx^m \quad (3.38)$$

Where $C_0, C_1, C_2$ etc. are the coefficients to be determined? The sum of the squares of the differences between the data points and corresponding values from the approximating polynomial is given by:

$$S = \sum_{i=1}^{n} [\, y_i - (C_0 + C_1x + C_2x^2 + C_3x^3 + \ \ldots\ldots\ldots\ldots\ldots + C_mx^m)]^2 \quad (3.39)$$

The minimum occurs when the partial derivatives of S with respect to $C_0, C_1, C_2$ etc. are all zero. This gives

$$\frac{\partial S}{\partial C_0} = 0; \quad \frac{\partial S}{\partial C_1} = 0; \quad \frac{\partial S}{\partial C_2} = 0; \ldots\ldots\ldots\ldots \quad \frac{\partial S}{\partial C_m} = 0 \quad (3.40)$$

The equations may be further simplified in the form of

$$\sum y_i - \sum c_0 - \sum c_1 x_i - \sum c_2 x_i^2 - \ \ldots\ldots\ldots\ldots\ldots \sum c_m x_i^m = 0 \tag{3.41}$$

$$\sum x_i y_i - c_0 \sum x_i - c_1 \sum x_i^2 - c_2 \sum x_i^3 - \ \ldots\ldots\ldots\ldots\ldots - c_m \sum x_i^{m+1} = 0 \tag{3.42}$$

$$\sum x_i^m y_i - c_0 \sum x_i^m - c_1 \sum x_i^{m+1} - c_2 \sum x_i^{m+2} - \ \ldots\ldots\ldots\ldots\ldots - c_m \sum x_i^{2m} = 0 \tag{3.43}$$

Or, the equations may be written in the form of

$$n \sum c_0 + c_1 \sum x_i + c_2 \sum x_i^2 + \ \ldots\ldots\ldots\ldots\ldots + c_m \sum x_i^m = \sum y_i \tag{3.44}$$

$$c_0 \sum x_i + c_1 \sum x_i^2 + c_2 \sum x_i^3 + \ \ldots\ldots\ldots\ldots\ldots + c_m \sum x_i^{m+1} = \sum x_i y_i \tag{3.45}$$

$$c_0 \sum x_i^m + c_1 \sum x_i^{m+1} + c_2 \sum x_i^{m+2} + \ \ldots\ldots\ldots\ldots\ldots + c_m \sum x_i^{2m} = \sum x_i^m y_i \tag{3.46}$$

Where all the summations are over n data points, i.e. i=1 to i=n

In case of two independent variables the equations reduce to:

$$n \sum c_0 + c_1 \sum x_{1,i} + c_2 \sum x_{2,i} = \sum y_i \tag{3.47}$$

$$c_0 \sum x_{1,i} + c_1 \sum x_{1,i}^2 + c_2 \sum x_{1,i} x_{2,i} = \sum x_i y_i \tag{3.48}$$

$$c_0 \sum x_{2,i} + c_1 \sum x_{1,i} x_{2,i} + c_2 \sum x_{2,i}^2 = \sum x_i^m y_i \tag{3.49}$$

Several important non polynomial forms of the function for curve fitting can be linearized so that the methods of linear regression can be applied. Among these, the most common forms are exponential and power-law variations, which may be defined as

$$f(x) = Ae^{ax} \quad f(x) = Bx^b \tag{3.50}$$

The corresponding linearized forms are given by, respectively,

$$\ln[\mathrm{f(x)}] = \ln(A) + ax \tag{3.51}$$

$$\ln[\mathrm{f(x)}] = \ln(B) + b\ln x \tag{3.52}$$

where ln (*x*) represents the natural logarithm of *x*. In these two cases, if a dependent variable *Y* is defined as *Y* = ln [ *f*(*x*)] and an independent variable *X* as *X* = *x* in the first case and *X*= ln(*x*) in the second, then the two equations become linear in terms of *X* and *Y*. These equations may be written as *Y* = *C* + *DX* and linear regression may be applied with the new variables *X* and *Y* to obtain the intercept *C*, which is ln(*A*) or ln(*B*), and the slope *D*, which is *a* or *b* for the two cases. Then, *A* or *B* is given by exp(*C*) and *a* or *b* by *D*. Therefore, from this linear fit, the constants *A*, *a*, *B*, and *b* can be calculated.

# Chapter 4

# Description of experimental setup

A Cross flow design is developed in which the air flow is directed perpendicular to the water flow. Air flow enters the cooling pad to meet water in cooling pad material. Water flows (perpendicular to the air) through the cooling pad by gravity. Gravity distributes the water uniformly across the pad material. Evaporative cooling of water and air occurs as air passes across the pad material. Water is circulated through a pump station and supplied to the top of the cooling pad via a distribution manifold. A distribution pad on the top of the cooling pad ensures an even water distribution. The water flows down the corrugated surface of the CELdek evaporative cooling pad. Part of the water is evaporated by the air that passes through the pad. The rest of the water assists in washing the pad, and is drained back to the pump station through a gutter system. The heat that is needed for the evaporation is taken from the air itself. The air that leaves the pad is therefore cooled and humidified simultaneously without any external energy supply for the evaporation process. This is nature's own cooling process.

## 4.1 Description of various parts of experimental setup:

4.1.1 Cellulose cooling pad
4.1.2 Air passage
4.1.3 Sprayer
4.1.4 Collecting tank
4.1.5 Instruments to measure data

### 4.1.1 Cellulose Cooling pad:

CELdek 7090 evaporative cooling pad is used in the test rig, which is used in systems where high efficiency cooling is required. It can be used for many different cooling purposes but is particularly suitable for evaporative coolers for commercial and domestic use. The pad consists of specially impregnated and corrugated cellulose paper sheets with different flute angles, one steep (45 deg) and one flat (15 deg) that have been bonded together.

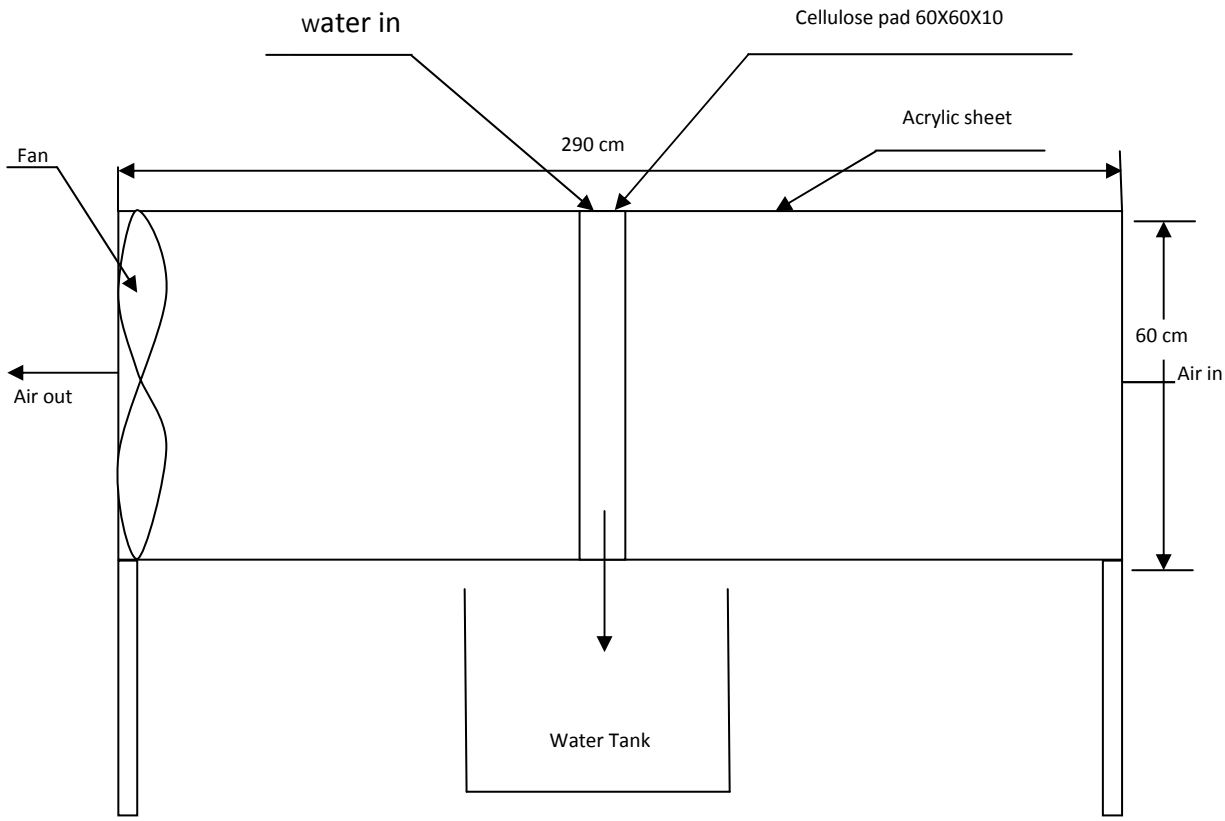


**Figure 4.1 Schematic line diagram of the evaporative cooling experimental setup**

**Front photograph of exp. setup**

**Side photograph of exp. setup**

**Photograph of Cellulose cooling pad used in evaporative cooling exp. setup**

This unique design yields a cooling pad with high evaporation efficiency while still operating with a very low pressure drop. In addition scaling is kept to a minimum and no water carry-over occurs due to the fact that the water is directed to the air inlet side of the pad. This is where most of the evaporation takes place. The impregnation procedure for the cellulose paper ensures a strong self supporting product, with high absorbance, which is protected against decomposition and rotting and therefore increasing longevity. Placed on top of the cooling pad it ensures a uniform supply of the water to the cooling pad and minimises the risk of dry spots.

Dimensions: Length: 60cm, Width: 60cm, Thickness: 10cm

### 4.1.2 Air passage:

The air passage of test rig is made of acrylic sheets of thickness 1cm. The passage cross section is square measuring 60cmX60cm. The length of passage is 290cm.

Size: 290cm x 60cm x 1cm

### 4.2.3 Sprayer:

Material: Galvanized steel (16 gauge)

Size: 60cm x 10cm x10cm

### 4.2.4 Collecting tank:

Size: 90cm x 60cm x 60cm

Material: Galvanized steel (16 Gauge)

### 4.2.5 Instruments to measure data

Air velocity:

Instrument: Anemometer, make: Lutron electronic enterprise company limited, Model: AM4201, Accuracy: ±2%

Temperature: Digital thermometer, Make: Mextech, Model: TM-1, Accuracy: $\pm.1^0$C

Relative humidity: Digital hygrometer, Make: Mextech, Model: TM-1, Accuracy: $\pm.1^0$C

# Chapter 5

# Experimental Investigations

## 5.1 Experimental procedure:

Variable parameters during experiments were air velocity, inlet water temperature and inlet air conditions. No attempts were made to control inlet air conditions, which is totally governed by environmental conditions. The inlet water temperature was selected in three ranges viz. (1) Normal water temperature (between DBT and WBT of inlet air) (2) Chilled water temperature (Below WBT of inlet air). (3) Elevated water temperature (above DBT of inlet air) other controllable parameters were air velocity and water mass flow rates. The velocity of air was measured at five locations of cooler exit cross section, one at centre and remaining four between centre and periphery with $90^0$ phase difference, and consequently average velocity was calculated. Range of face velocity is 4.7 to 13.54 m/s. Water mass flow rates measured were between 0.015 to 0.085 kg/s. At a particular time the inlet and outlet air conditions (DBT and RH) were measured simultaneously by digital hygrometers, whereas inlet and outlet water temperatures using digital thermometers. Total time of measurement of various readings for one observation was less than two minutes during which change in ambient conditions were found to be insignificant. In each set 5 sets of observations were taken.

## 5.2 Development of Mathematical expressions from experimental data:

The equations 5.1 through 5.13 are established through experimental data obtained. Polynomial and regression fits are used for curve fitting as discussed in chapter 3, formulations of evaporative cooling systems.

**5.2.1** Relationships between heat and mass transfer coefficient, mean temperature of air and velocity of air are given below for different water temperatures:

**(i) For normal water temperature:**

$$h_c = -3.57 \times 10^4 + 2.23 \times 10^3 T_m - 34.7 T_m^2 + 4.49 V_a + 0.19 V_a^2 \quad (5.1)$$

$$h_m = -3.45 \times 10^4 + 2.15 \times 10^3 T_m - 33.5 T_m^2 + 4.34 V_a + 0.18 V_a^2 \quad (5.2)$$

**(ii) For elevated water temperature:**

$$h_c = 3.53 \times 10^4 - 2.19 \times 10^3 T_m + 33.9 T_m^2 + 2.25 V_a + 0.319 V_a^2 \quad (5.3)$$

$$h_m = 3.43 \times 10^4 - 2.13 \times 10^3 T_m + 32.9 T_m^2 + 2.08 V_a + 0.308 V_a^2 \quad (5.4)$$

**(iii) For chilled water temperature:**

$$h_c = -2.14 \times 10^4 + 1.50 \times 10^3 T_m - 26.48 T_m^2 + 20.96 V_a - 0.182 V_a^2 \quad (5.5)$$

$$h_m = -2.05 \times 10^4 + 1.44 \times 10^3 T_m - 25.36 T_m^2 + 20.15 V_a - 0.175 V_a^2 \quad (5.6)$$

Where $h_c = Heat\ Transfer\ coefficient, h_m = Mass\ Transfer\ coefficient,\ T_m = Mean\ temperature\ of\ air\ flow, V_a = Velocity\ of\ air$

**5.2.2 Relationship between Nusselt, Reynold and prandtl numbers by polynomial fit:**

**(i) Normal water temperature**

$$Nu = 1.93 \times 10^7 + 1.72 \times 10^{-3} Re + 1.16 \times 10^{-8} Re^2 - 5.17 \times 10^7 \times Pr + 3.46 \times 10^7 Pr^2 \quad (5.7)$$

**(ii) Elevated water temperature**

$$Nu = -3.32 \times 10^6 + 4.48 \times 10^{-3} Re + 1.6 \times 10^{-8} Re^2 + 8.92 \times 10^6 \times Pr - 5.96 \times 10^7 Pr^2 \quad (5.8)$$

**(iii) Chilled water temperature**

$$Nu = 4.84 \times 10^{8} + 2.34 \times 10^{-2} Re - 8.96 \times 10^{-8} Re^{2} - 1.29 \times 10^{9} \times Pr + 8.65 \times 10^{8} Pr^{2} \quad (5.9)$$

### 5.2.3 Relationship between Nusselt, Reynold and prandtl numbers by regression analysis:

$$N_u = C(R_e)^a (Pr)^b \quad (5.10)$$

**(i) For normal water temperature**

$C = 6.44 \times 10^{-21}$ , $a = 0.7873$ , $b = -149.0588$

**(ii) For elevated water temperature**

$C = 1.242 \times 10^{-30}$ , $a = 1.8143$ , $b = -189.3256$

**(iii) For chilled water temperature**

$C = 6.218 \times 10^{-28}$ , $a = 0.8073$ , $b = -208.2679$

### 5.3 Combined for the system (All water temperature):

The mathematical relations can be developed for the system combined i.e. as a whole, when system working on any of the water temperatures discussed above.

**(i) Heat and mass transfer coefficients:**

$$h_c = 6.28 \times 10^{3} - 3.74 \times 10^{2} T_m + 5.54 T_m^{2} + 12.2 V_a - 3.45 \times 10^{-2} V_a^{2} \quad (5.11)$$

$$h_m = 6.10 \times 10^{3} - 3.64 \times 10^{2} T_m + 5.39 T_m^{2} + 11.7 V_a - 3.38 \times 10^{-2} V_a^{2} \quad (5.12)$$

**(ii) Relationship between Nusselt, Reynold and prabdtl numbers:**

$$Nu = 1.63 \times 10^{7} + 5.58 \times 10^{-3} Re + 7.19 \times 10^{-9} Re^{2} + 4.34 \times 10^{7} \times Pr - 2.89 \times 10^{7} Pr^{2} \quad (5.13)$$

**(iii) Relationship between Nusselt, Reynold and prandtl numbers by regression analysis:**

$N_u = C(R_e)^a(Pr)^b$

$C = 5.73 \times 10^{-16}$ , $a = 1.1396$ , $b = -98.2885$

**5.4 Mathematical modelling of the system on computer:** A mathematical model is developed for the processes using Academic version of EES software, to predict outlet air temperature, outlet air humidity, heat and mass transfer coefficients, water evaporation rate, cooling efficiency, humidifying efficiency, dew point effectiveness and wet bulb effectiveness. Graphs are plotted for various variables measured experimentally and compared with model results, using EES parametric tables.

To test and verify the adequacy of the suggested mathematical model and program, the theoretical results from the mathematical model was compared with the experimental data, to make sure that the results of the mathematical model program are accurate. The comparison shows that theoretical results are very close to the results obtained by experiments, as compared and tabulated in table no's 1 through 18 in Appendix-I. Therefore, the developed model has satisfactory adequacy and can be successfully used in designing works of direct evaporative coolers.

For evaluating the performance of the experimental test rig graphs are plotted between various performance parameters (cooling efficiency, humidifying efficiency, wet bulb effectiveness, dew point effectiveness etc.) and the measurable quantities (velocity of air flow, inlet air temperature, change in DBT, change in water temperature etc.). To develop relationship between variables viz. water flow rate, air flow rate, change in temperature of air, curve fitting of various data obtained through experiments is done, using regression analysis, which tells about the relationship among dependent and independent variables involved in the process.

# Chapter 6

# Results and discussions

Based upon the formulations developed in chapter 3 and mathematical modelling of the evaporative cooling system on computer, the following results out need be discussed. The discussion is divided into three parts based upon the temperature of water entering the system. Figures 6.1 through 6.34 show the variation of different performance parameter with change in the measurable parameter. Graphs have been plotted to compare the model and experimental results.

### 6.1 Normal water temperature:

The temperature of water flowing through the wet cooling media is in the range of 23 to $29^0$C, whereas that of environmental incoming air is in the range of 34 to $35^0$C. The experimental results show a temperature drop in the range of 3 to $5^0$C, for different air to water flow ratios. The air flow velocities ranging from 4.7 to 13.54m/s, whereas water flow rate ranging from 0.015 to 0.085 kg/s. The drop in temperature of water measured in the range of 2 to $2.5^0$C. The performance parameters are cooling efficiency, humidifying efficiency, wet bulb effectiveness and dew point effectiveness. Figures 6.1 through 6.15 conclude the performance of the system.

#### 6.1.1 The drop in DBT:

The variation of change in DBT of air with change in velocity of air at different mass flow rates of water is shown in figure 6.1. The trend is of decrease in DBT drop with increase in velocity of air, i.e. increase in outlet temperature for same inlet temperature with increase in air velocity, which is due to air to water contact time. It is clear from the figure that change in DBT per unit change in air flow rate is maximum at maximum water flow rate and minimum at minimum water flow rates.

**Table 1: Experimental Inlet and outlet dry bulb temperatures and relative humidity at Normal water temperature, m_w=0.015 kg/s at different air velocities**

| $M_w$ =0.015 kg/s | | | | | | |
|---|---|---|---|---|---|---|
| $V_a$ (m/s) | $T_{air}$ (DBT $^0$C) | | $T_{water}$($^0$C) | | Rel. Hum. (%) | |
| | IN | OUT | IN | OUT | IN | OUT |
| 4.70 | 34.4 | 30.8 | 28 | 26 | 45 | 72 |
| 5.90 | 34.4 | 31.1 | 27.5 | 25.5 | 44 | 70 |
| 8.20 | 34.4 | 31.2 | 27.5 | 25.5 | 44 | 68 |
| 10.60 | 34.5 | 31.4 | 27.5 | 25.5 | 44 | 67 |
| 13.54 | 34.6 | 31.5 | 27.5 | 25.5 | 44 | 66 |

**Table 2: Experimental Inlet and outlet dry bulb temperatures and relative humidity at normal water temperature, m_w=0.050 kg/s at different air velocities**

| $M_w$ =0.050 kg/s | | | | | | |
|---|---|---|---|---|---|---|
| $V_a$ (m/s) | $T_{air}$ (DBT $^0$C) | | $T_{water}$($^0$C) | | Rel. Hum. (%) | |
| | IN | OUT | IN | OUT | IN | OUT |
| 4.70 | 34.6 | 30.4 | 27 | 25 | 44 | 69 |
| 5.90 | 34.5 | 30.5 | 26.5 | 24.5 | 44 | 68 |
| 8.20 | 34.4 | 30.6 | 26 | 24 | 44 | 65 |
| 10.60 | 34.4 | 30.8 | 25.5 | 23.5 | 44 | 64 |
| 13.54 | 34.7 | 31 | 25.5 | 23.5 | 44 | 63 |

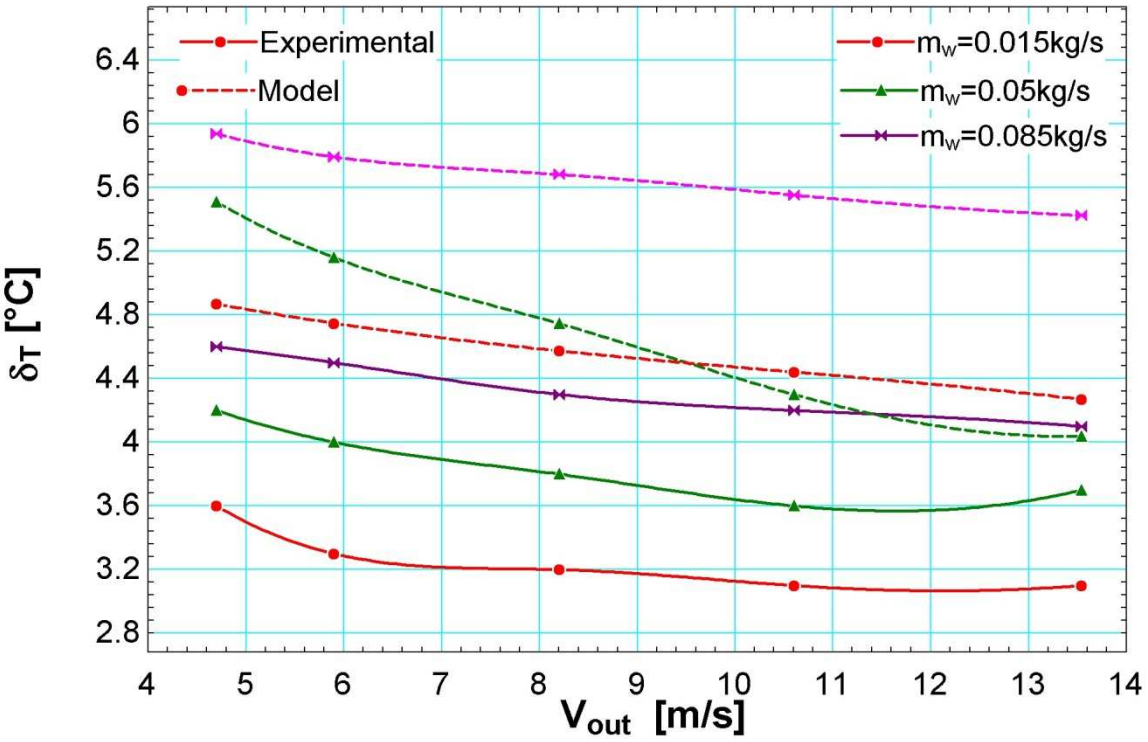


**Figure 6.1 Variation of delta T with change in velocity of air for normal water temperature at different water flow rates**

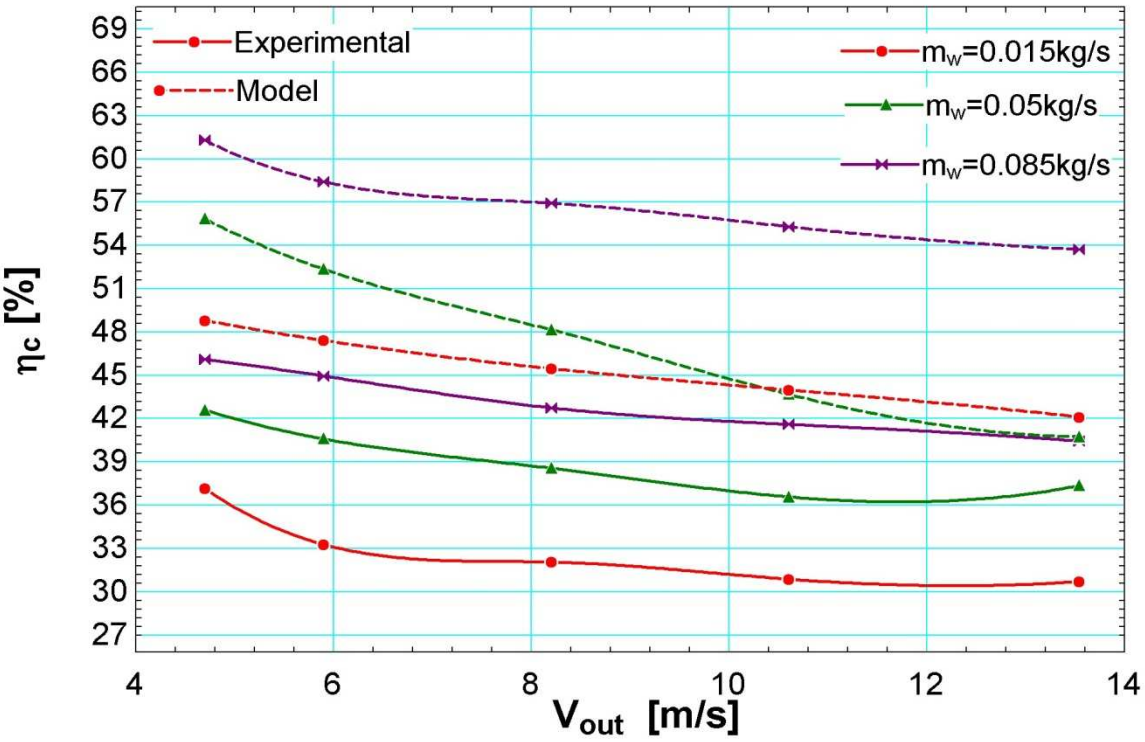


**Figure 6.2 Variation of cooling efficiency with change in velocity of air for normal water temperature at different water flow rates**

### 6.1.2 Cooling efficiency:

The variation of cooling efficiency with change in velocity of air for at different mass flow rates of water is shown in figure 6.2. The trend is of decrease in cooling efficiency with increase in velocity of air, which is due to air to water contact time. The experimental cooling efficiency ranges from 35 to 45%.

Figure 6.3 depicts the comparison of model and experimental variation of change in humidity ratio of air at different mass flow rates of water. The trend is of more change in humidity with more water flow rates. Deviation from the trend, at some instants is due to change in inlet air conditions.

The comparison of model and experimental variation of change in DBT of air for normal water temperature at different mass flow rates of water is shown in figure 6.4. The experimental values validate the model for almost all cases.

Figure 6.5 depicts the variation in Water evaporation rate with change in air flow rate at different water flow rates. The trend is of increase water evaporation rate with increase in air flow rate, which is due to more and more mass flow rate of air. Water evaporation rate shows very less variation with water flow rate.

### 6.1.3 Dew point effectiveness:

The variation in dew point effectiveness with change in air velocities at different water flow rates is shown in figure 6.6. The trend is of decrease in dew point effectiveness with increase in air velocity, which is due to less and less time of contact of air with water with higher air velocities. The fit used in the diagram is cubic fit, which deviates from the trend, at some instants which is due to change in inlet air conditions. The experimental dew point effectiveness varies from 0.25 to 0.35.

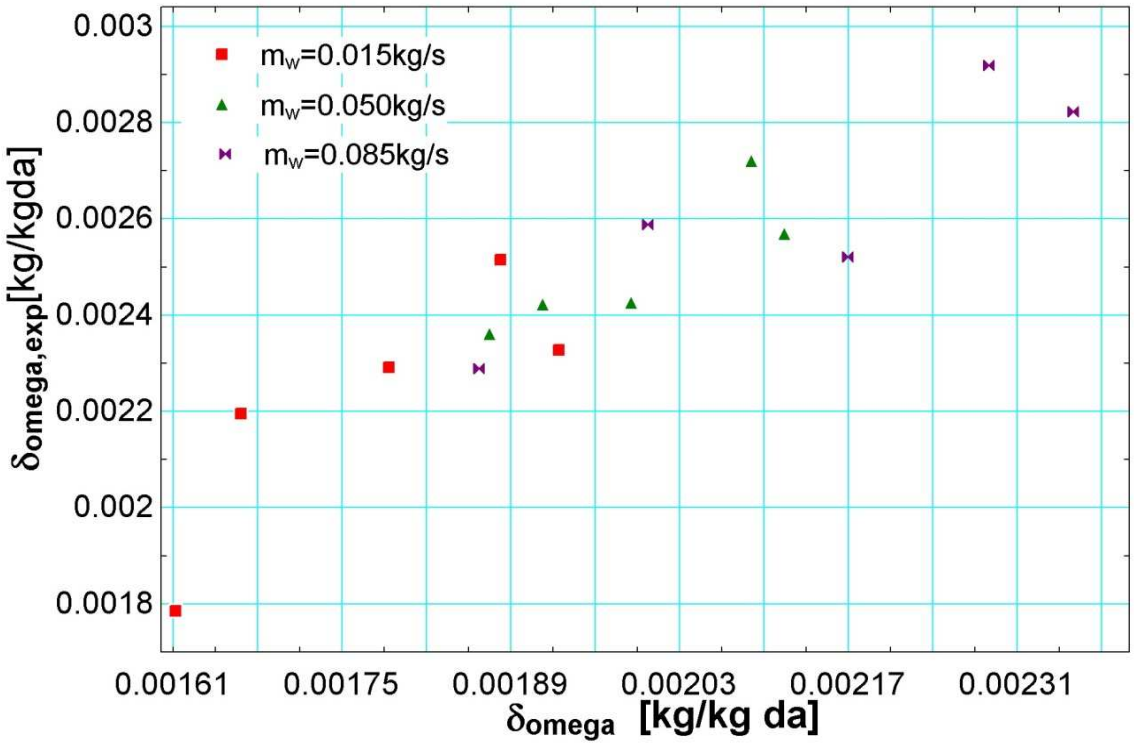


**Figure 6.3 Humidity ratio change model V/s experimental at different water flow rates**

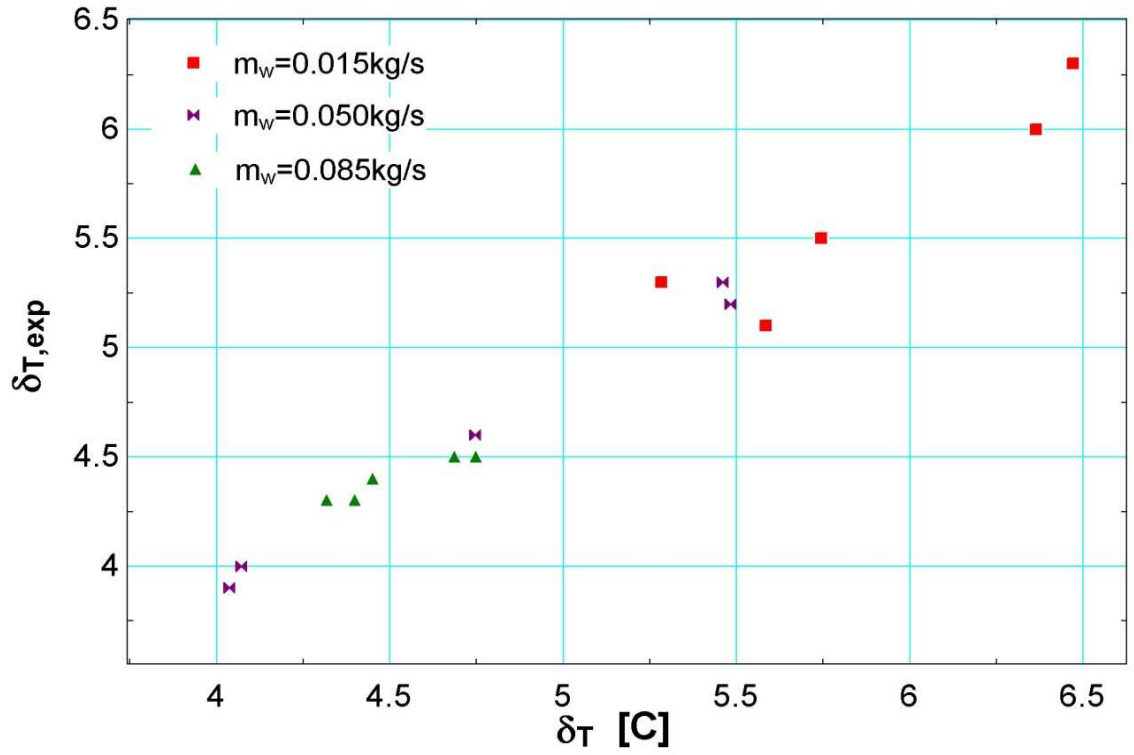


**Figure 6.4 Change in temperature of air model V/s experimental at different water flow rates**

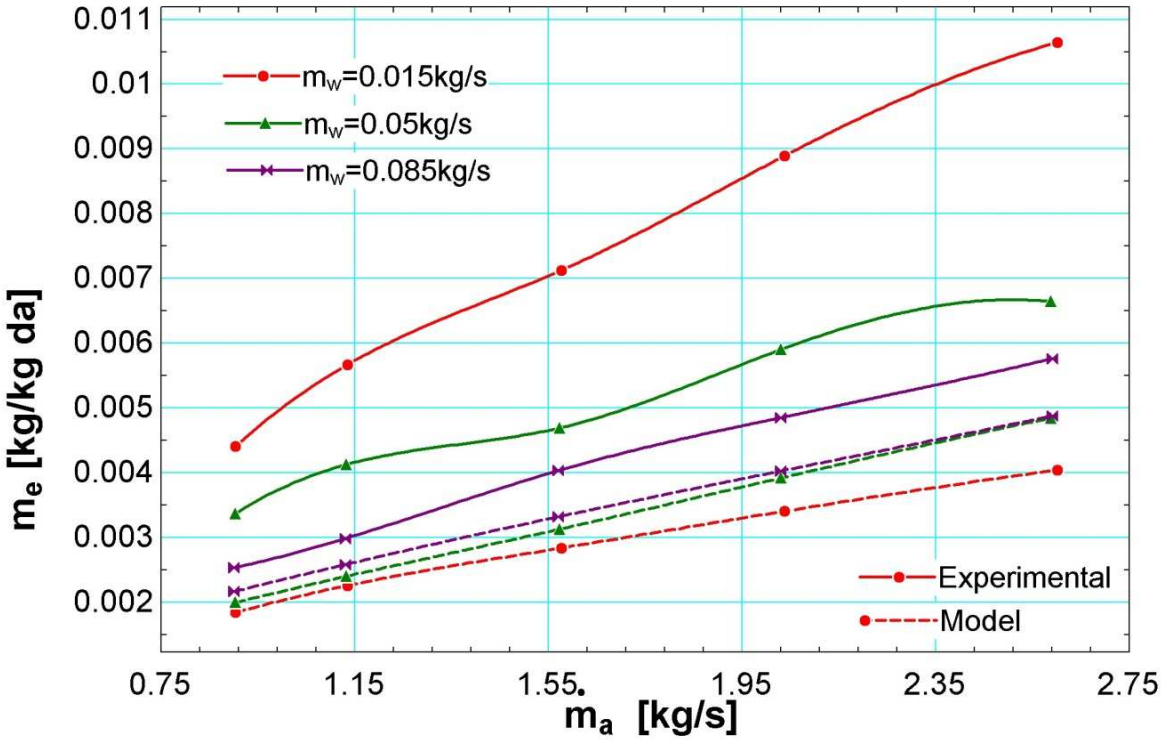


**Figure 6.5 Variation in Water evaporation rate with change in air flow rate at different water flow rates**

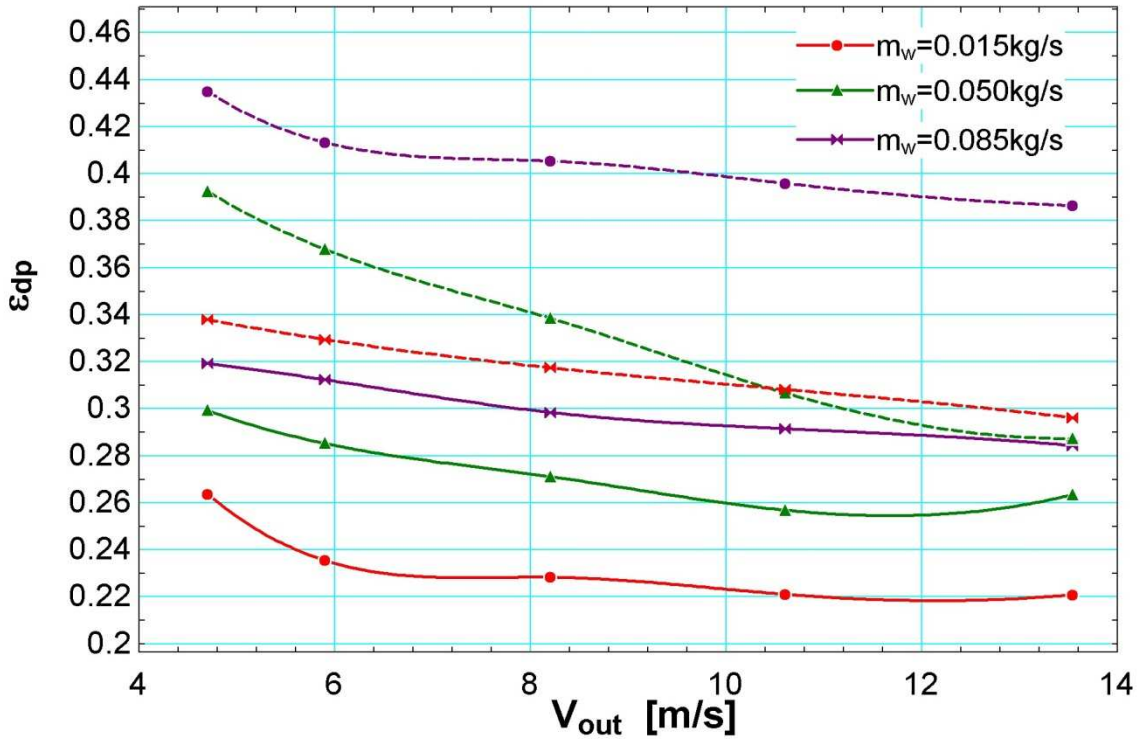


**Figure 6.6 Variation in dew point effectiveness with air velocity at different water flow rates**

**Table 2: Experimental Inlet and outlet dry bulb temperature and relative humidity at normal water temperature, m_w=0.085 kg/s at different air velocities**

| $M_w$ =0.085 kg/s | | | | | | |
|---|---|---|---|---|---|---|
| $V_a$ (m/s) | $T_{air}$ (DBT $^0$C) | | $T_{water}$($^0$C) | | Rel. Hum. (%) | |
| | IN | OUT | IN | OUT | IN | OUT |
| 4.70 | 34.6 | 30 | 25.5 | 23.5 | 43 | 66 |
| 5.90 | 34.6 | 30.1 | 25.5 | 23.5 | 43 | 65 |
| 8.20 | 34.6 | 30.3 | 25.5 | 23.5 | 43 | 64 |
| 10.60 | 34.6 | 30.4 | 25.5 | 23.5 | 43 | 63 |
| 13.54 | 34.7 | 30.6 | 25.5 | 23.5 | 43 | 62 |

**Table 4: Comparison of Experimental and model data for normal water temperature m_w=0.015 kg/s at different air velocities**

| $M_w$ =0.015 kg/s | | | | | | | | |
|---|---|---|---|---|---|---|---|---|
| $V_a$ (m/s) | $T_{air,in}$ (DBT$^0$C) | RH in (%) | $T_{air,out}$(DBT$^0$C) | | | Rel. Hum.$_{out}$ (%) | | |
| | | | Model | Exp. | Error | Model | Exp. | Error |
| 4.70 | 34.4 | 45 | 28.46 | 30.8 | 2.34 | 71.2 | 72 | 0.8 |
| 5.90 | 34.4 | 44 | 28.61 | 31.1 | 2.49 | 69 | 70 | 1 |
| 8.20 | 34.4 | 44 | 28.72 | 31.2 | 2.48 | 67.8 | 68 | 0.2 |
| 10.60 | 34.5 | 44 | 28.95 | 31.4 | 2.42 | 66.7 | 67 | 0.3 |
| 13.54 | 34.6 | 44 | 29.18 | 31.5 | 2.32 | 65.8 | 66 | 0.2 |

**Table 5:3 Comparison of Experimental and model data for normal water temperature m_w=0.050 kg/s at different air velocities**

| $M_w$ =0.050 kg/s | | | | | | | | |
|---|---|---|---|---|---|---|---|---|
| $V_a$ (m/s) | $T_{air,in}$ ($DBT^0C$) | $RH_{in}$ (%) | $T_{air,out}$($DBT^0C$) | | | Rel. $Hum._{out}$ (%) | | |
| | | | Model | Exp. | Error | Model | Exp. | Error |
| 4.70 | 34.6 | 44 | 29.09 | 30.4 | 1.31 | 68.6 | 69 | 0.2 |
| 5.90 | 34.5 | 44 | 29.34 | 30.5 | 1.16 | 66.9 | 68 | 1.1 |
| 8.20 | 34.4 | 44 | 29.66 | 30.6 | 0.94 | 64.9 | 65 | 0.1 |
| 10.60 | 34.4 | 44 | 30.1 | 30.8 | 0.7 | 63 | 64 | 1 |
| 13.54 | 34.7 | 44 | 30.66 | 31 | 0.34 | 61.8 | 63 | 1.2 |

**Table 6: Comparison of Experimental and model data for normal water temperature m_w=0.085 kg/s at different air velocities**

| $M_w$ =0.085 kg/s | | | | | | | | |
|---|---|---|---|---|---|---|---|---|
| $V_a$ (m/s) | $T_{air,in}$ ($DBT^0C$) | $RH_{in}$ (%) | $T_{air,out}$($DBT^0C$) | | | Rel. $Hum._{out}$ (%) | | |
| | | | Model | Exp. | Error | Model | Exp. | Error |
| 4.70 | 34.6 | 43 | 29.73 | 30 | 0.23 | 65.5 | 66 | 0.5 |
| 5.90 | 34.6 | 43 | 29.85 | 30.1 | 0.25 | 64.6 | 65 | 0.4 |
| 8.20 | 34.6 | 43 | 30.03 | 30.3 | 0.27 | 63.4 | 64 | 0.6 |
| 10.60 | 34.6 | 43 | 30.16 | 30.4 | 0.24 | 62.1 | 63 | 0.9 |
| 13.54 | 34.7 | 43 | 30.43 | 30.6 | 0.17 | 61.4 | 62 | 0.6 |

Figure 6.7 depicts comparison of experimental dew point effectiveness versus model results at different water flow rates. The results shown in figure depict very less deviation of experimental results from that one of the model.

The variation of dew point effectiveness with Inlet air temperature at different water flow rates is shown in figure 6.8. The trend is of decreased dew point effectiveness with increase in temperature. Results shown in figure depict very less deviation of experimental results from that one of the model.

### 6.1.4 Wet bulb effectiveness:

The wet bulb effectiveness variation with change in air velocities at different water flow rates is shown in figure 6.9. The trend is of decrease in wet bulb effectiveness with increase in velocity, which is due to less and less time of contact of air with water with higher air velocities. The experimental wet bulb effectiveness ranges from 0.30 to 0.45.

Figure 6.10 depicts variation of wet bulb effectiveness with Inlet air temperature at different water flow rates. The trend is of decreased wet bulb effectiveness with increase in temperature. Figure 6.11 depicts comparison of wet bulb effectiveness at normal water temperature, experimental versus model results at different water flow rates. The results shown in figure depict very less deviation of experimental results from that one of the model.

### 6.1.5 Humidifying efficiency:

The variation of humidifying efficiency with air velocity at different water flow rates is shown in figure 6.12. The obvious result from figure is that humidifying efficiency decreases with increase in velocity and decrease in water flow rate. The inlet conditions i.e. DBT, WBT affect the outlet condition hence the humidifying efficiency of the cooling system.

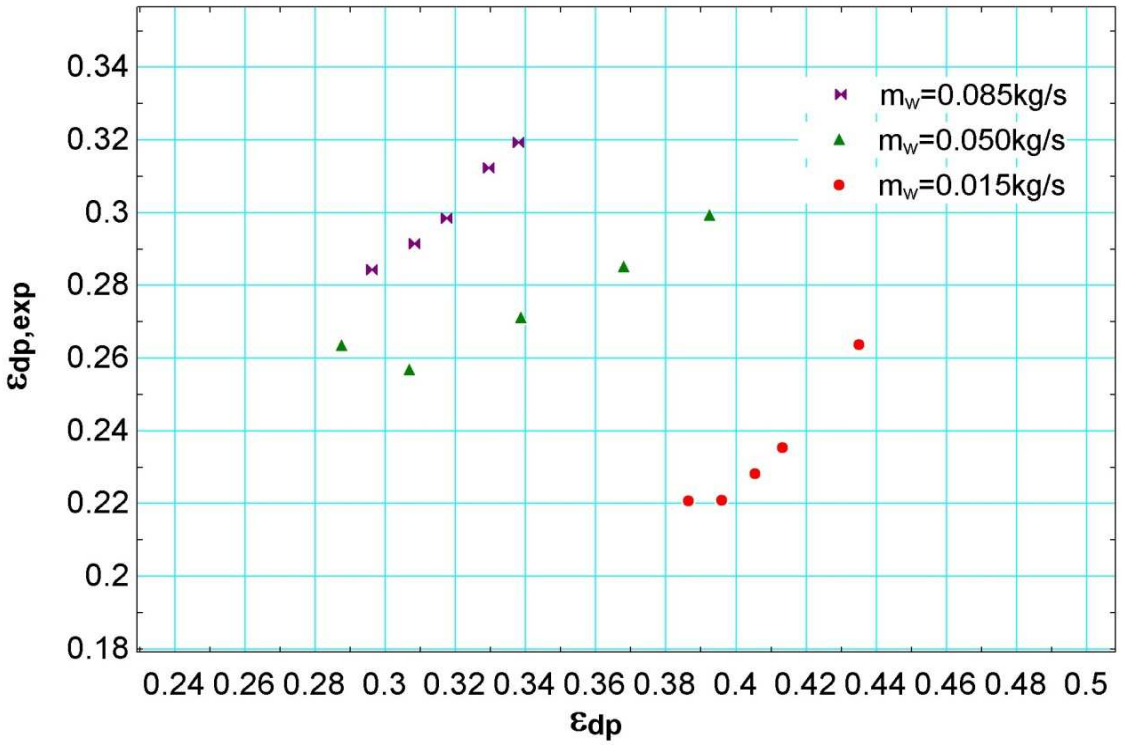


**Figure 6.7 Dew point effectiveness Experimental V/s model at different water flow rates**

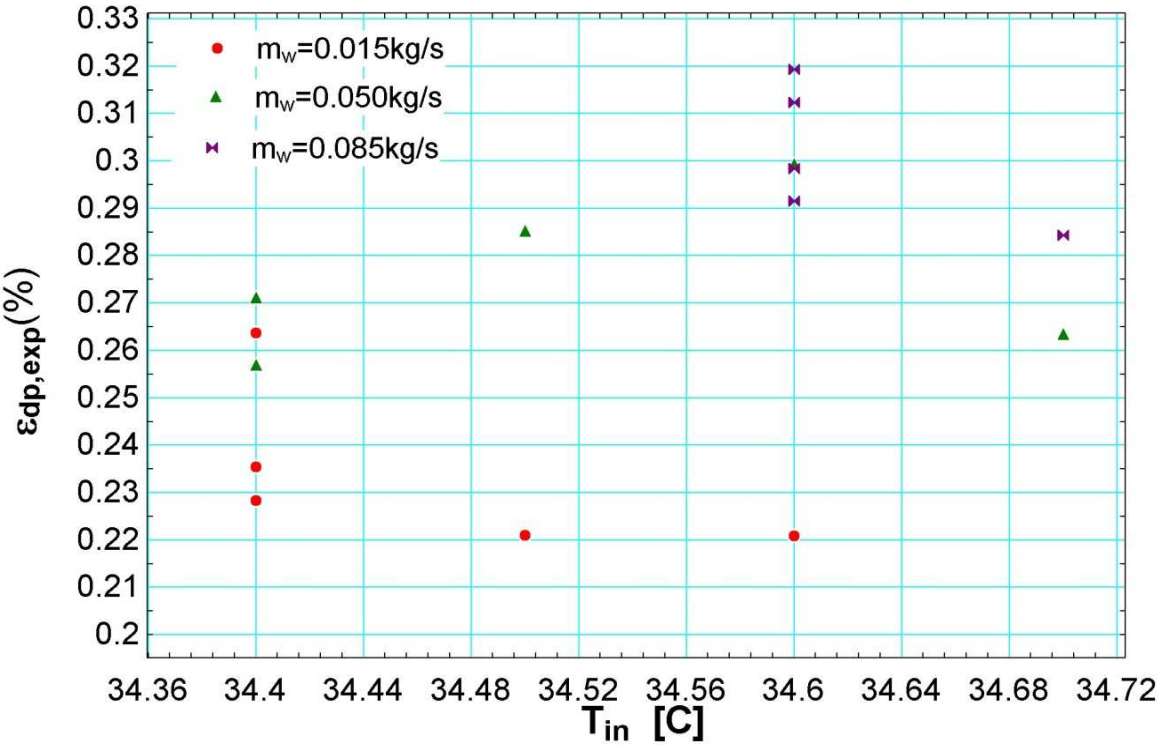


**Figure 6.8 Variation of Dew point effectiveness with Inlet air temperature at different water flow rates**

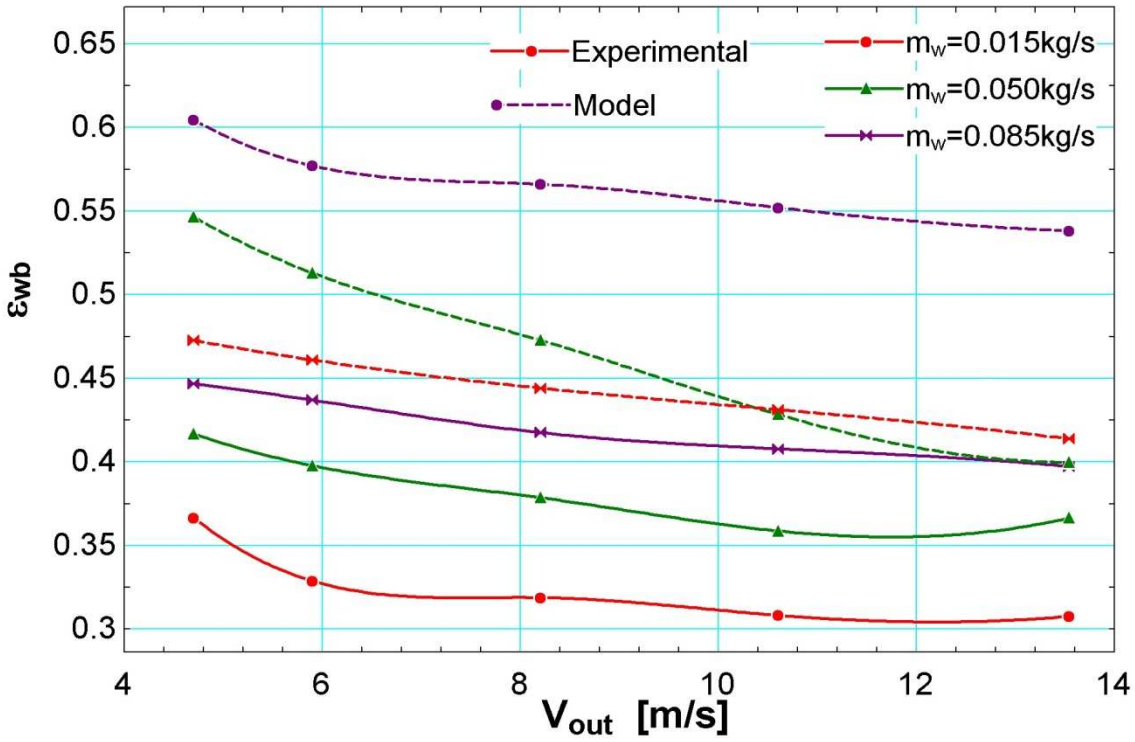


**Figure 6.9 Variation of wet bulb effectiveness with air velocity at different water flow rates**

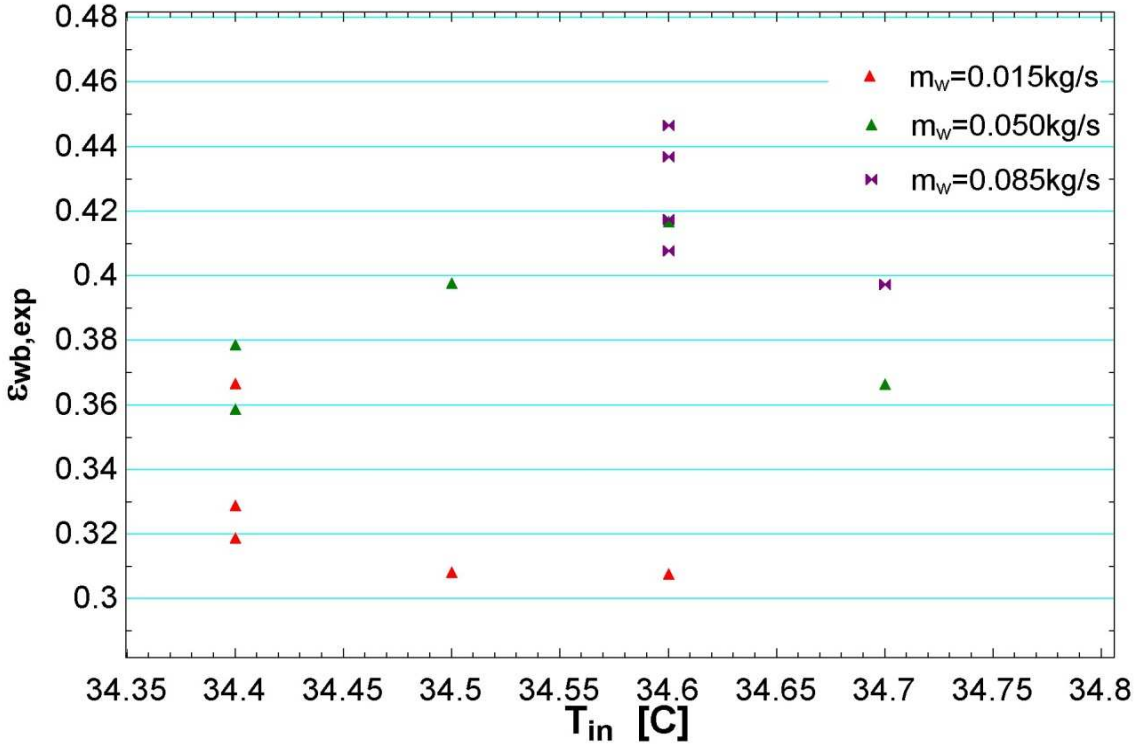


**Figure 6.10 Variation of wet bulb effectiveness with Inlet temperature of air at different water flow rates**

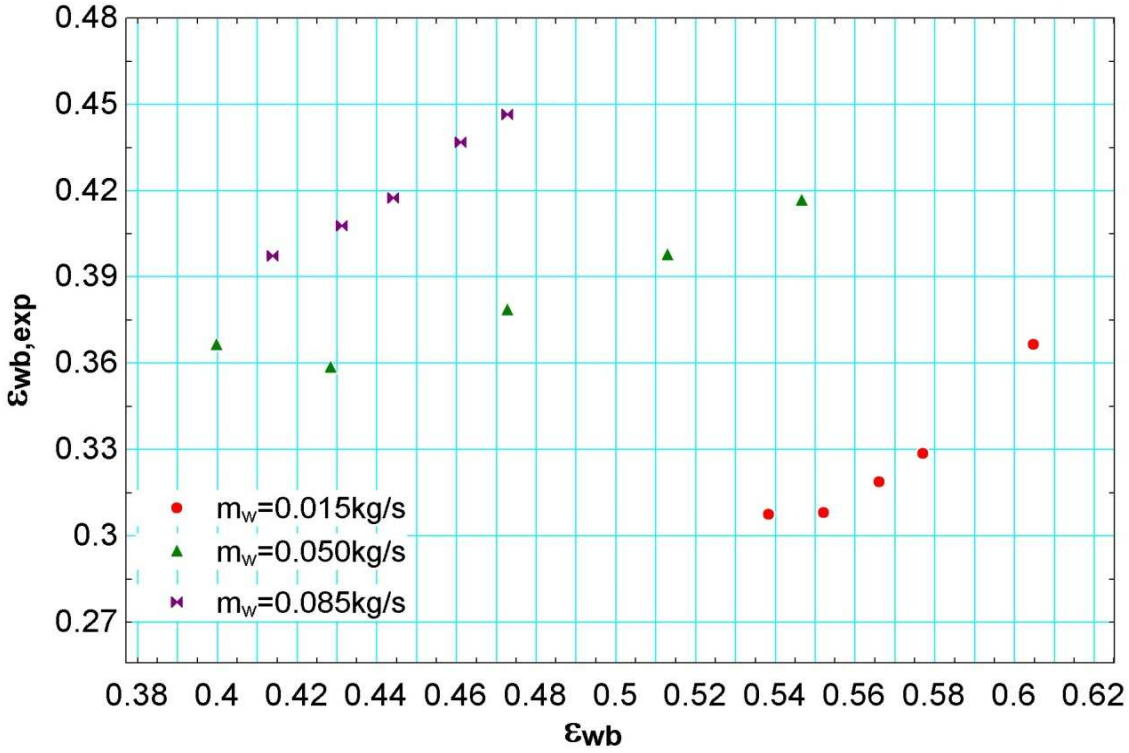


**Figure 6.11 Comparison of wet bulb effectiveness experimental versus model at different water flow rates**

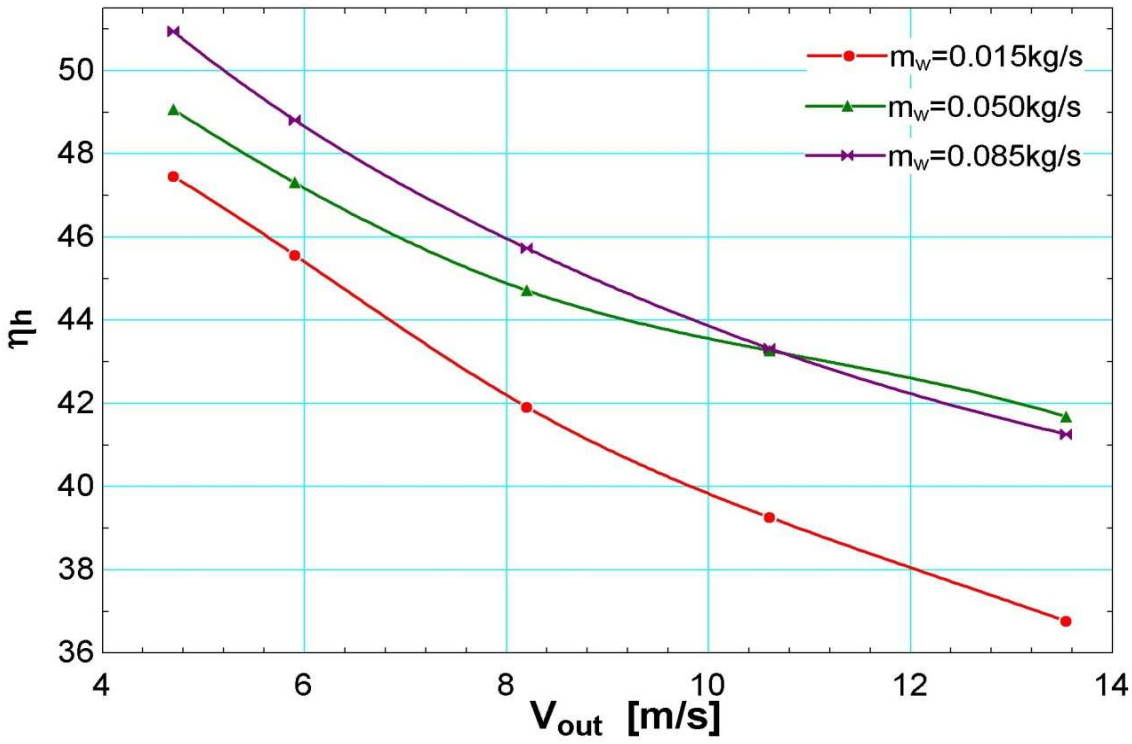


**Figure 6.12 Variation of humidifying efficiency with Air velocity at different water flow rates**

### 6.1.6 Exergy destruction and exergetic efficiency:

There is a destruction of exergy of the flowing air in evaporative cooling systems. The graphs 6.13 and 6.14 show the variation of exergy destruction and exergetic efficiency with variation of velocity of air. The deviation from trend is due to variation in the inlet conditions of air.

### 6.1.7 Heat transfer coefficient:

Heat transfer coefficient increases with increase in velocity of air as is obvious from figure 6.15. Heat transfer coefficient is a function of velocity of air and mean temperature of the air. It also increases with increase in mass flow rate of water as is shown in figure 6.15.

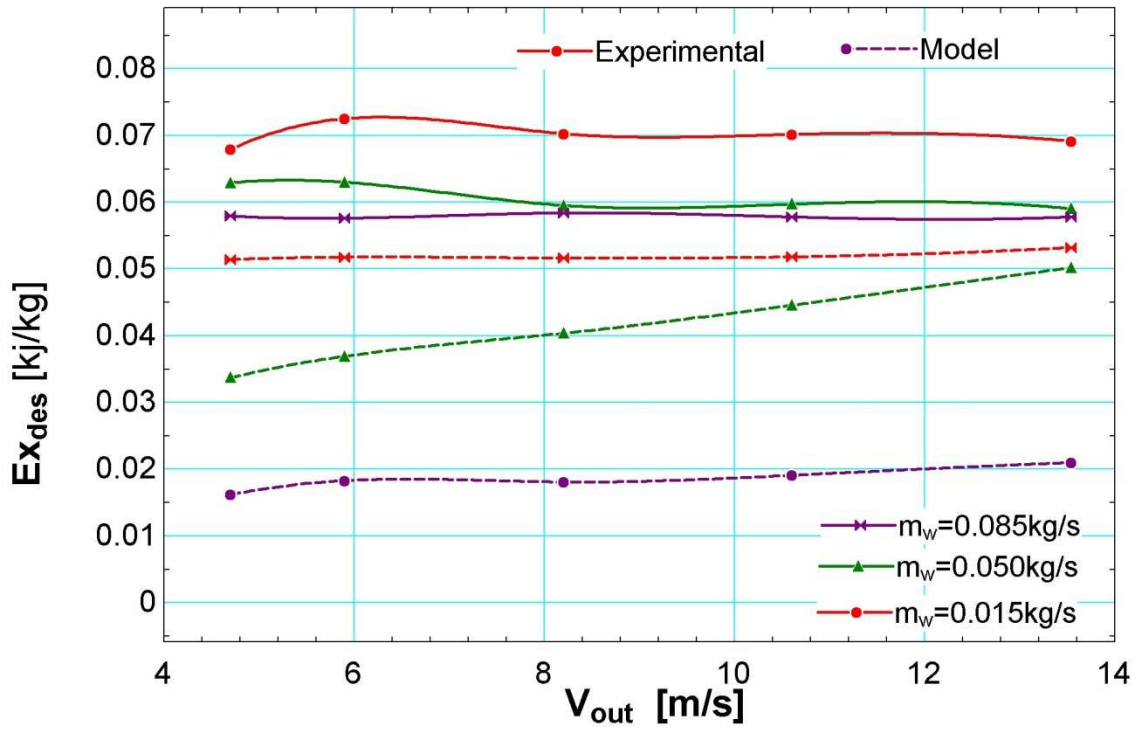


**6.13 Variation of exergy destruction with change in air velocity at different water flow rates**

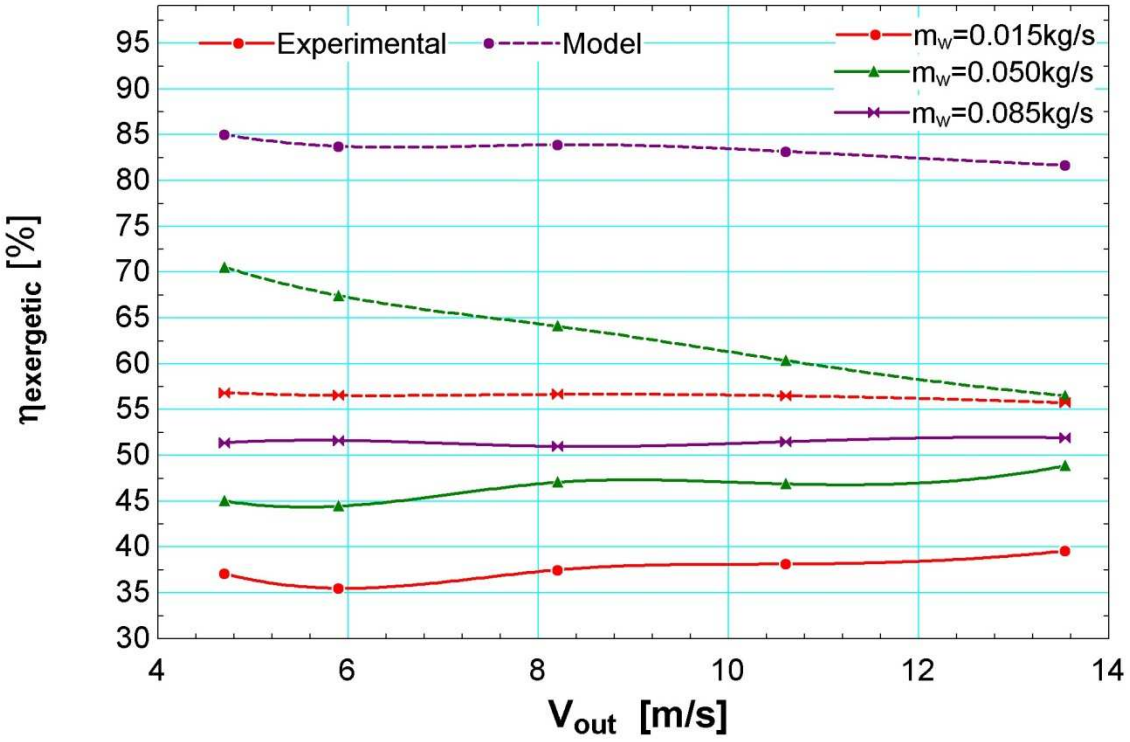


**6.14 Variation of exergetic efficiency with change in air velocity at different water flow rates**

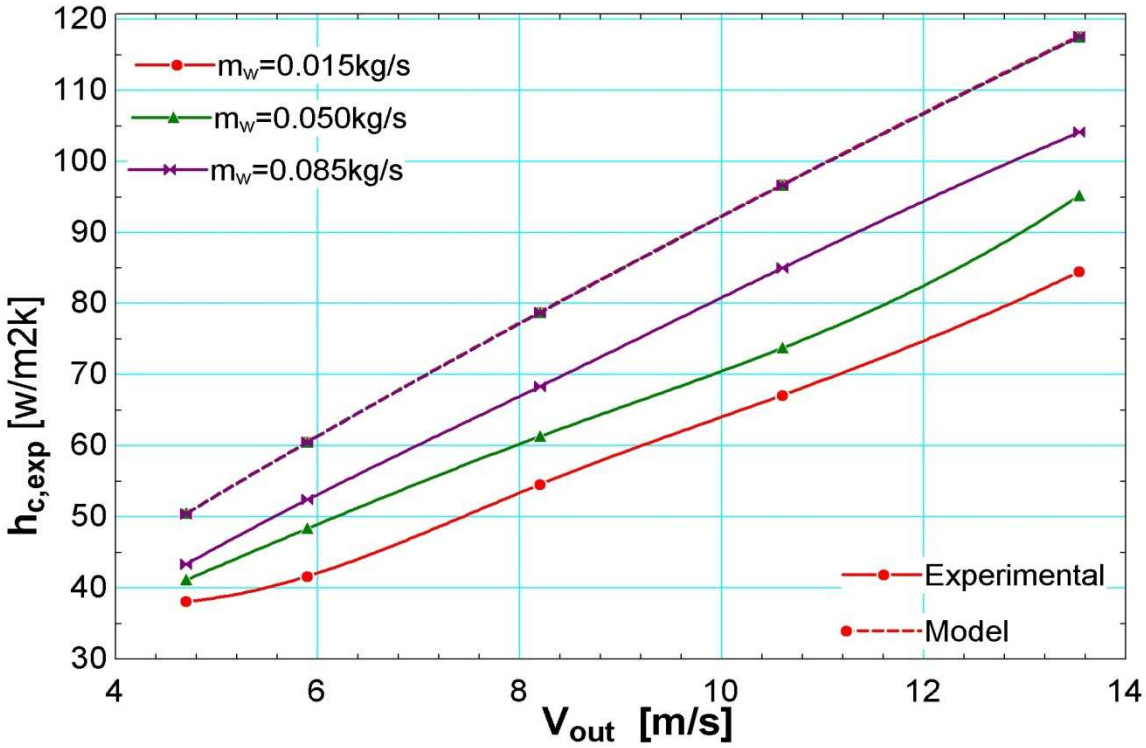


**Figure 6.15 Variation of heat transfer coefficient with velocity of air at different water flow rates**

**6.2 Elevated water temperature:**

The water temperature selected was above DBT of air, in the range of 45 to $52^0$ C. The water evaporates at higher rate for same inlet conditions as compared to normal water temperature. The system serves as a cross flow cooling tower. Both air and water are cooled due to evaporation of water.

A mathematical model based on energy balance across the cooling pad is developed for the processes using Academic version of EES software, to predict outlet air temperature, outlet air humidity, heat and mass transfer coefficients, water evaporation rate, cooling efficiency, humidifying efficiency, dew point effectiveness and wet bulb effectiveness. Graphs were plotted for various variables measured experimentally and compared with model results, using EES parametric table.

To test and verify the adequacy of the suggested mathematical model and program, the theoretical results from the mathematical model is compared with the experimental data, to make sure that the results of the mathematical model program are accurate. The comparison shows that theoretical results are very close to the results obtained by experiments. Therefore, the developed model has satisfactory adequacy and can be successfully used in designing works of cross flow cooling tower.

The graphs plotted between various measurable and modelled parameters, show negligible difference between measured and model values. For evaluating the performance of the experimental test rig graphs are plotted between various performance parameters and the measurable quantities. To develop relationship between variables viz. water flow rate, air flow rate, change in temperature of air, curve fitting of various data obtained through experiments is done, using regression analysis, which tells about the relationship among dependent and independent variables involved in the process.

### 6.2.1 Change in DBT of air:

Figure 6.16 depicts the change in DBT of air with change in air velocity at different water flow rates. DBT change is less for higher velocities of air, as the temperature of water is more than DBT of air and for higher velocities there is less time for heat exchange; hence outlet temperature is lower as compared to those at lower velocities. DBT change is less for higher mass flow rates of water due to higher inter-surface area at higher mass flow rates of water hence outlet temperature will be more at higher mass flow rates of water, as is depicted by the figure. The experimental DBT change varies from 1.5 to $4.5^0$C.

The DBT change with respect to velocity trend, in case of elevated water temperatures is opposite to that in case of normal or chilled water. Also the DBT change with respect to water flow is also opposite to that in case of normal or chilled water.

### 6.2.2 Drop in water temperature:

Water temperature drop with change in velocity of air at different mass flow rates of water is shown in figure 6.17. The experimental change in temperature is in the range of 17 to $24^0$C. This large drop in temperature is due to high temperature of water due to which less heat is required to evaporate the water. There is not much variation in water temperature drop across the media for a single mass flow rate of water. The trend is of increasing water temperature for decreasing mass flow rate of water, also there is a deviation from the trend due to sudden inlet water temperature change.

Variation of Change in specific humidity with velocity of air different water flow rates is shown in figure 6.18. The specific humidity change decreases with increase in velocity and vice-versa. Also there is a trend of increasing change in specific humidity change with increasing mass flow rate.

**Table 7:4 Experimental Inlet and outlet dry bulb temperatures and relative humidity at elevated water temperature, m_w=0.015 kg/s at different air velocities**

| $M_w$ =0.015 kg/s | | | | | | |
|---|---|---|---|---|---|---|
| $V_a$ (m/s) | $T_{air}$ (DBT $^0$C) | | $T_{water}$($^0$C) | | Rel. Hum. (%) | |
| | IN | OUT | IN | OUT | IN | OUT |
| 4.70 | 32.7 | 29.7 | 46.2 | 26 | 49 | 79 |
| 5.90 | 32.8 | 29.4 | 46.2 | 27.5 | 49 | 78 |
| 8.20 | 32.8 | 28.9 | 46.4 | 28 | 49 | 76 |
| 10.60 | 32.8 | 28.7 | 46.4 | 28.5 | 52 | 76 |
| 13.54 | 32.8 | 28.7 | 46.4 | 29 | 52 | 75 |

**Table 8: Experimental Inlet and outlet dry bulb temperatures and relative humidities at elevated water temperature, m_w=0.050 kg/s at different air velocities**

| $M_w$ =0.050 kg/s | | | | | | |
|---|---|---|---|---|---|---|
| $V_a$ (m/s) | $T_{air}$ (DBT $^0$C) | | $T_{water}$($^0$C) | | Rel. Hum. (%) | |
| | IN | OUT | IN | OUT | IN | OUT |
| 4.70 | 32.8 | 30.1 | 51 | 27.1 | 55 | 92 |
| 5.90 | 32.9 | 29.7 | 51 | 26.5 | 55 | 88 |
| 8.20 | 32.9 | 29.2 | 51 | 26.1 | 55 | 86 |
| 10.60 | 32.8 | 28.8 | 50.4 | 26.2 | 55 | 84 |
| 13.54 | 32.7 | 28.7 | 50.2 | 26.2 | 55 | 83 |

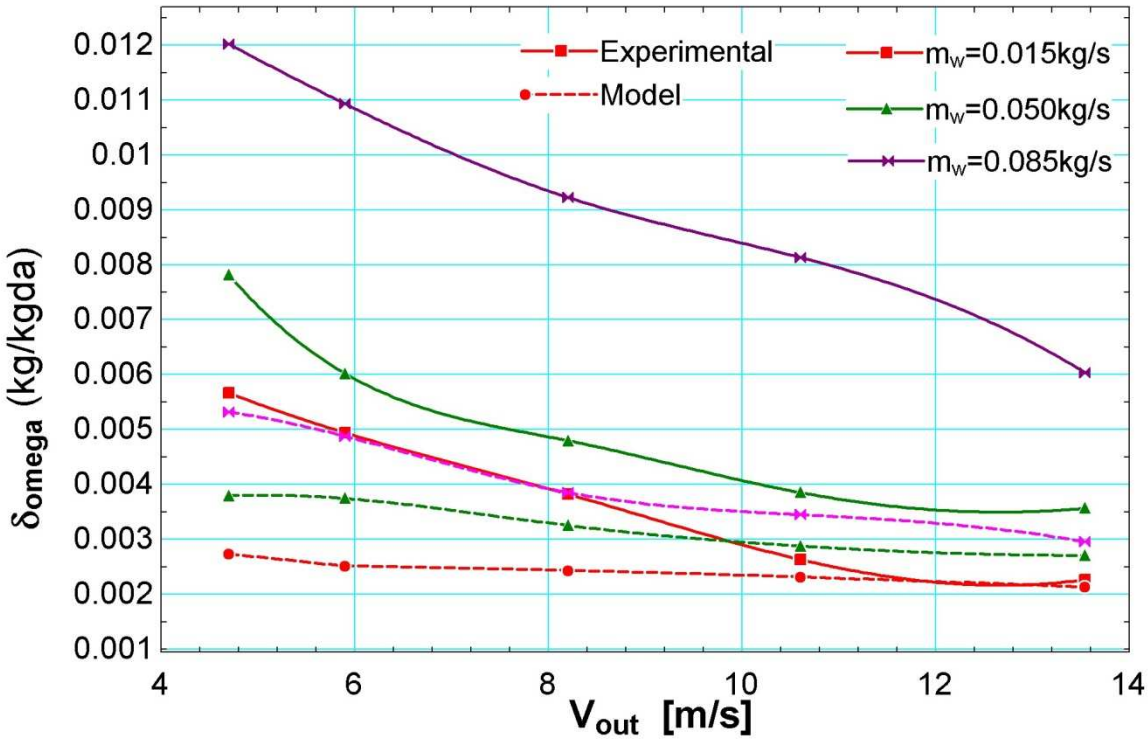


**Figure 6.16 Variation of Change in specific humidity versus Velocity of air for elevated water temperature at different water flow rates**

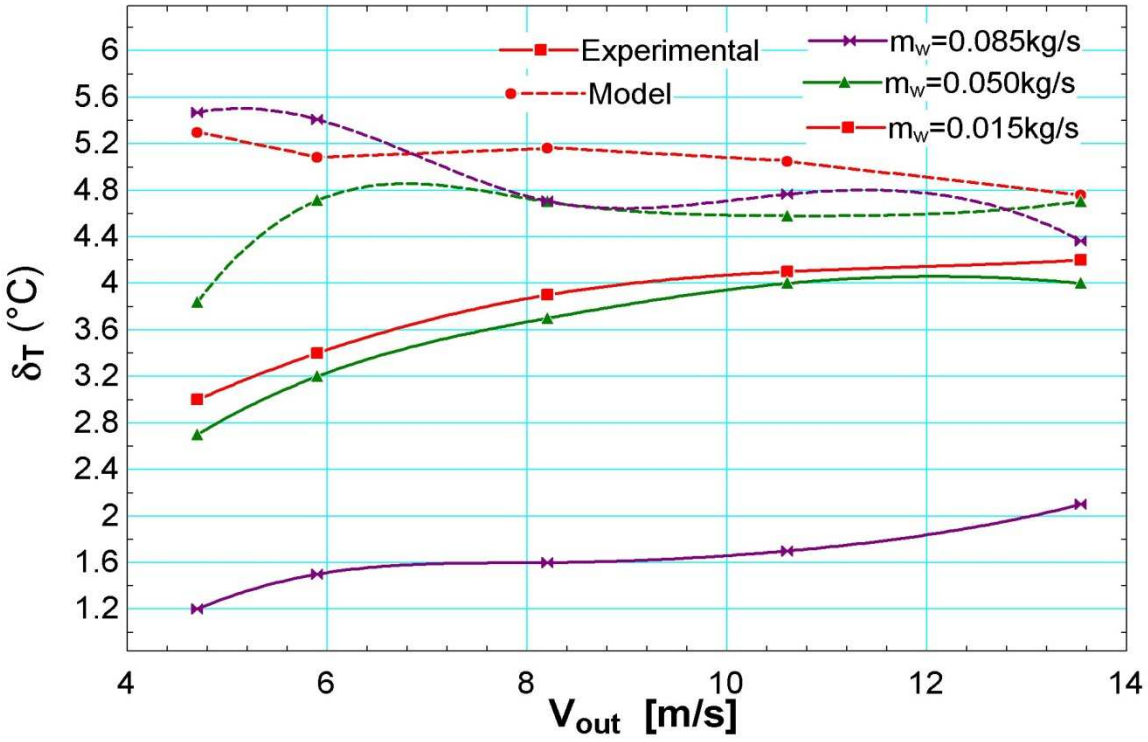


**Figure 6.17 Variation of Change in DBT of air versus Velocity of air for elevated water temperature at different water flow rates**

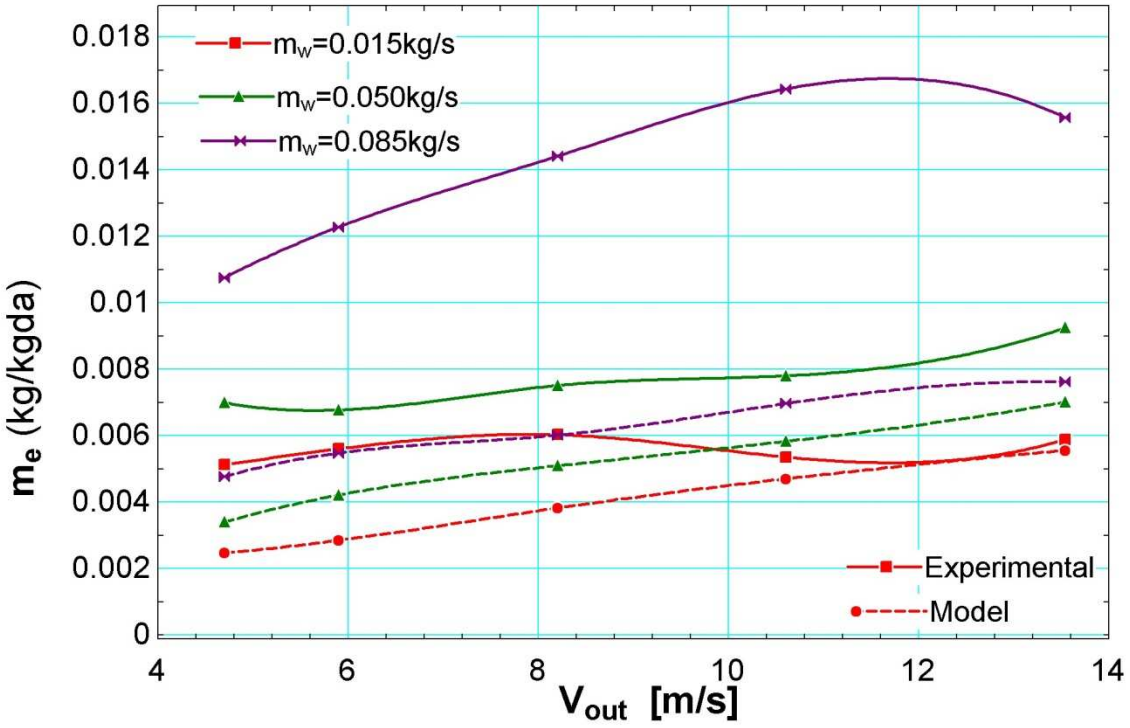


**Figure 6.18 Variation of water evaporation rate versus Velocity of air for elevated water temperature at different water flow rates**

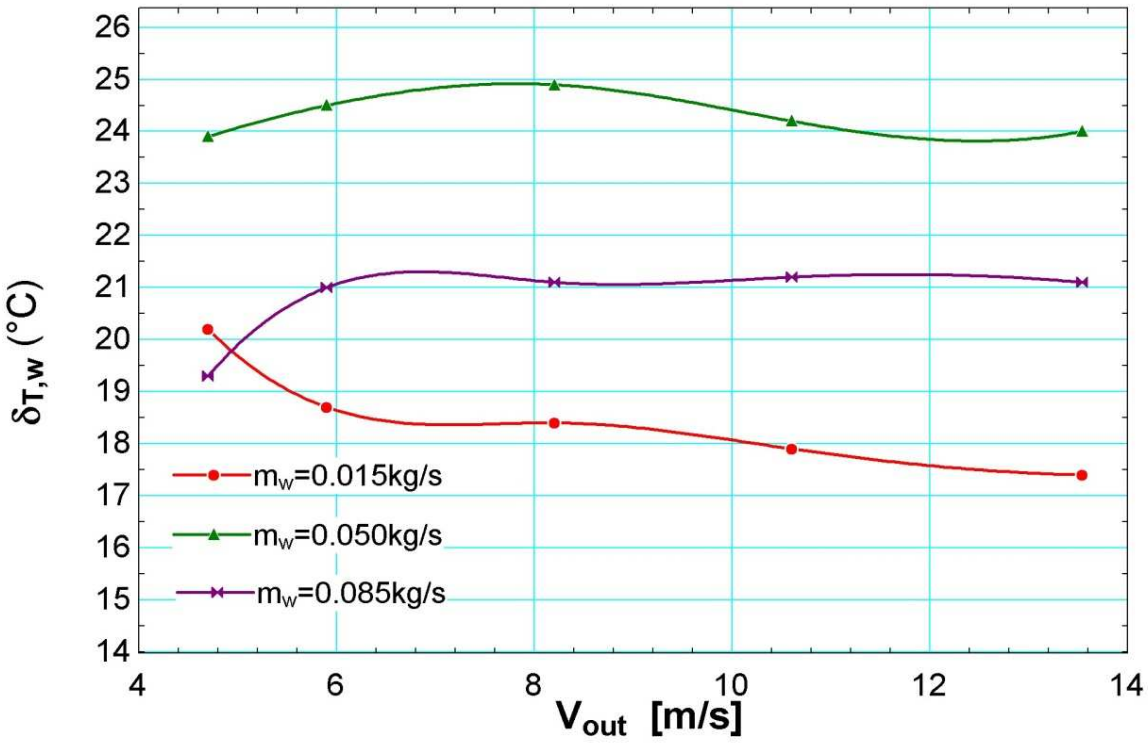


**Figure 6.19 Variation of Change in water temperature versus Velocity of at different water flow rates**

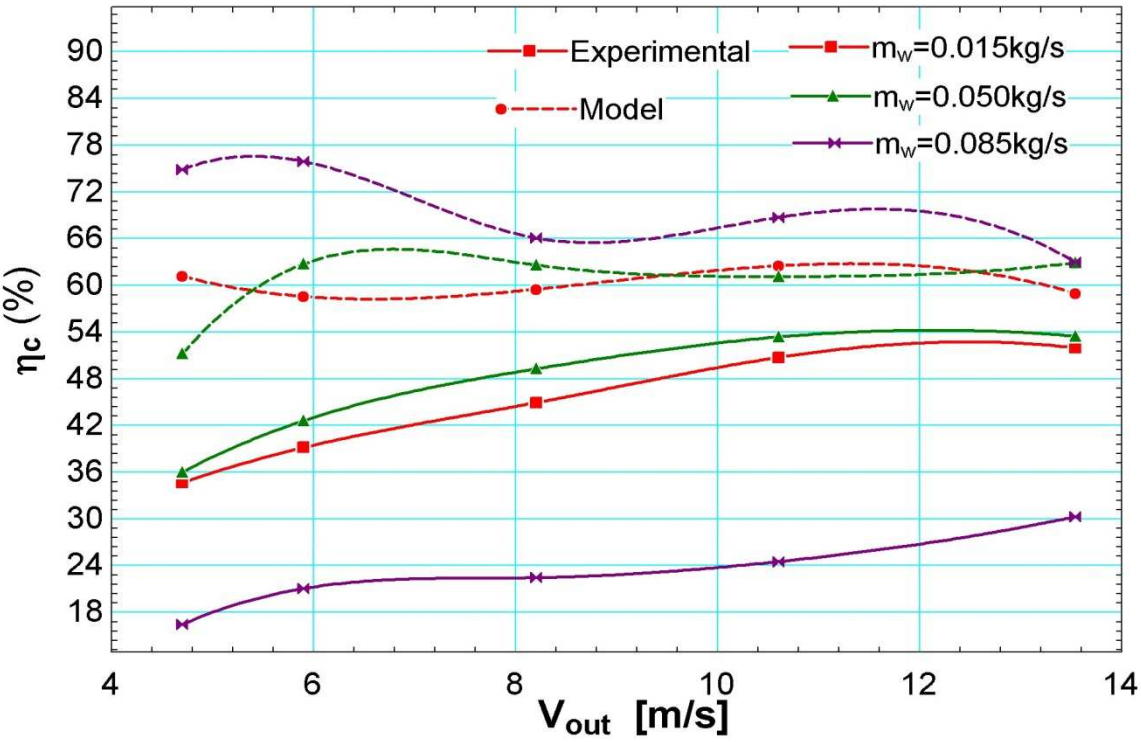


**Figure 6.20 Variation of cooling efficiency versus Velocity of air at different water flow rates**

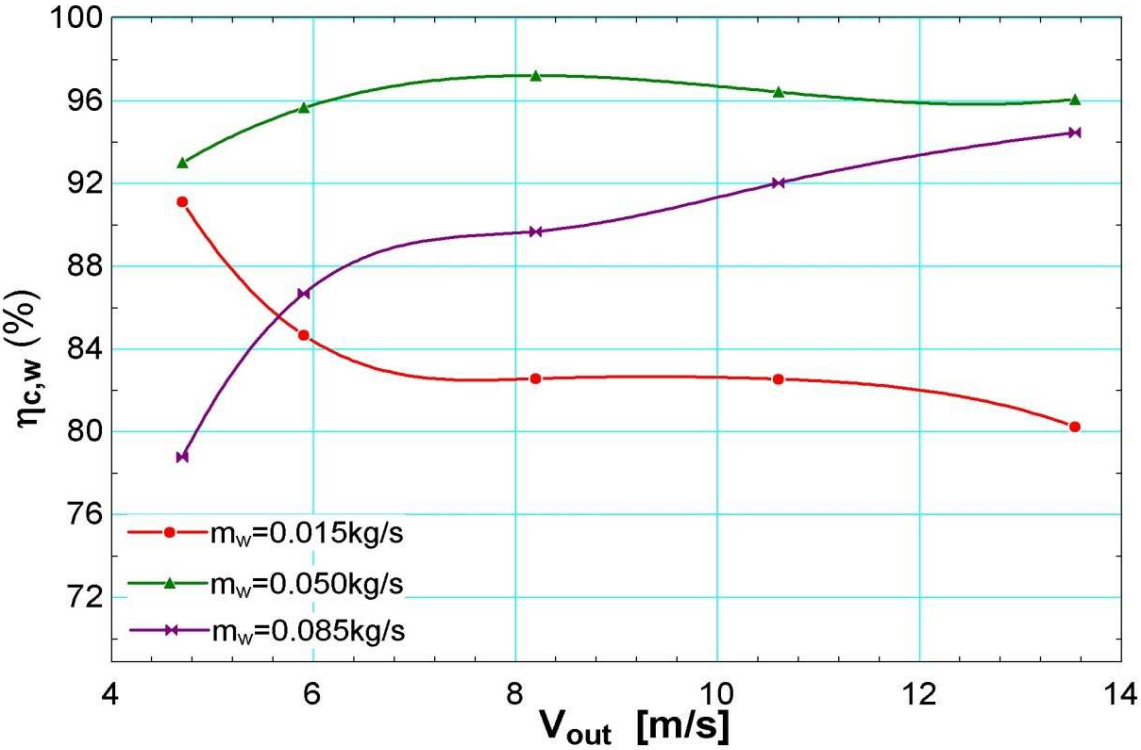


**Figure 6.21 Variation of water cooling efficiency versus Velocity of air at different water flow rates**

**Table 9: Experimental Inlet and outlet dry bulb temperatures and relative humidity at elevated water temperature, m_w=0.085 kg/s at different air velocities**

| $M_w$ =0.085 kg/s | | | | | | |
|---|---|---|---|---|---|---|
| $V_a$ (m/s) | $T_{air}$ (DBT $^0$C) | | $T_{water}$($^0$C) | | Rel. Hum. (%) | |
| | IN | OUT | IN | OUT | IN | OUT |
| 4.70 | 32.8 | 31.6 | 50 | 30.7 | 56 | 99 |
| 5.90 | 32.9 | 31.4 | 50 | 29 | 57 | 98 |
| 8.20 | 32.9 | 31.3 | 49.3 | 28.2 | 57 | 93 |
| 10.60 | 32.9 | 31.2 | 49 | 27.8 | 58 | 91 |
| 13.54 | 32.9 | 30.8 | 48.3 | 27.2 | 58 | 86 |

**Table 10: Comparison of Experimental and model data for elevated water temperature m_w=0.015 kg/s at different air velocities**

| $M_w$ =0.015 kg/s | | | | | | | | |
|---|---|---|---|---|---|---|---|---|
| $V_a$ (m/s) | $T_{air,in}$ (DBT$^0$C) | Rel. Hum.$_{in}$ (%) | $T_{air,out}$(DBT$^0$C) | | | Rel. Hum.$_{out}$ (%) | | |
| | | | Model | Experimental | Difference | Model | Experiment | Difference |
| 4.70 | 32.7 | 49 | 27.4 | 29.7 | 2.3 | 78 | 79 | 1 |
| 5.90 | 32.8 | 49 | 27.71 | 29.4 | 1.69 | 76 | 78 | 2 |
| 8.20 | 32.8 | 49 | 27.64 | 28.9 | 1.26 | 76 | 76 | 0 |
| 10.60 | 32.8 | 52 | 27.75 | 28.7 | 0.95 | 79 | 76 | -3 |
| 13.54 | 32.8 | 52 | 28.04 | 28.7 | 0.66 | 77 | 75 | -4 |

**Table 11: Comparison of Experimental and model data for elevated water temperature m_w=0.050 kg/s at different air velocities**

| $M_w$ =0.050 kg/s | | | | | | | | |
|---|---|---|---|---|---|---|---|---|
| $V_a$ (m/s) | $T_{air,in}$ ($DBT^0C$) | Rel. $Hum._{in}$ (%) | $T_{air,out}$($DBT^0C$) | | | Rel. $Hum._{out}$ (%) | | |
| | | | Model | Experimental | Difference | Model | Experiment | Difference |
| 4.70 | 32.8 | 55 | 28.96 | 30.1 | 1.14 | 93 | 92 | -1 |
| 5.90 | 32.9 | 55 | 28.19 | 29.7 | 1.51 | 87 | 88 | 1 |
| 8.20 | 32.9 | 55 | 28.2 | 29.2 | 1 | 85 | 86 | 1 |
| 10.60 | 32.8 | 55 | 28.22 | 28.8 | 0.58 | 83 | 84 | 1 |
| 13.54 | 32.7 | 55 | 27.99 | 28.7 | 0.71 | 83 | 83 | 0 |

**Table 12: Comparison of Experimental and model data for elevated water temperature m_w=0.085 kg/s at different air velocities**

| $M_w$ =0.085 kg/s | | | | | | | | |
|---|---|---|---|---|---|---|---|---|
| $V_a$ (m/s) | $T_{air,in}$ ($DBT^0C$) | Rel. $Hum._{in}$ (%) | $T_{air,out}$($DBT^0C$) | | | Rel. $Hum._{out}$ (%) | | |
| | | | Model | Experimental | Difference | Model | Experiment | Difference |
| 4.70 | 32.8 | 56 | 27.33 | 31.6 | 4.27 | 99 | 99 | 0 |
| 5.90 | 32.9 | 57 | 27.49 | 31.4 | 3.91 | 98 | 98 | 0 |
| 8.20 | 32.9 | 57 | 28.19 | 31.3 | 3.11 | 90 | 93 | 3 |
| 10.60 | 32.9 | 58 | 28.13 | 31.2 | 3.07 | 90 | 91 | 1 |
| 13.54 | 32.9 | 58 | 28.53 | 30.8 | 2.27 | 88 | 86 | -2 |

Variation of water evaporation rate with velocity of air at different water flow rates is shown in figure 6.19. The water evaporation rate increases with increase in velocity of air and vice-versa. This is due to the fact that the increased velocity means more mass flow rates of air hence although delta omega decreases with velocity still water evaporation rate per kg of dry air increases. Also water evaporation rate increases with increase in water flow rate as it increases the inter-surface contact area of air and water.

### 6.2.3 Cooling efficiency:

Cooling efficiency increases with increase in velocity of air as is shown in figure 6.20. Higher the time of contact with elevated temperature water with air, higher the air outlet temperature, hence lower the cooling efficiency that is what happens when air velocity is low. For a higher air velocity cooling efficiency increases. Also the cooling efficiency increases with decreasing the water mass flow rate. The experimental cooling efficiency ranges from 17 to 53%.

Figure 6.21 shows variation of water cooling efficiency versus velocity of air at different water flow rates. Water temperature drop with change in velocity of air at different mass flow rates of water is shown in figure 6.17. The large drop in water temperature shows high water cooling efficiency. There is not much variation in water cooling efficiency for a single mass flow rate of water. The trend is of increasing water cooling efficiency for decreasing mass flow rate of water, also there is a deviation from the trend due to sudden inlet water temperature change. The experimental water cooling efficiency ranges from 78-95%.

### 6.2.4 Exergy destruction and exergetic efficiency:

There is a destruction of exergy of the flowing air in evaporative cooling systems. The graphs 6.22 and 6.23 show the variation of exergy destruction and exergetic efficiency with variation of velocity of air. The deviation from trend is due to variation in the inlet conditions of air.

### 6.2.5 Heat transfer coefficient:

Heat transfer coefficient increases with increase in velocity of air as is obvious from figure 6.24. Heat transfer coefficient is a function of velocity of air and mean temperature of the air. It also increases with increase in mass flow rate of water as is shown in figure 6.15.

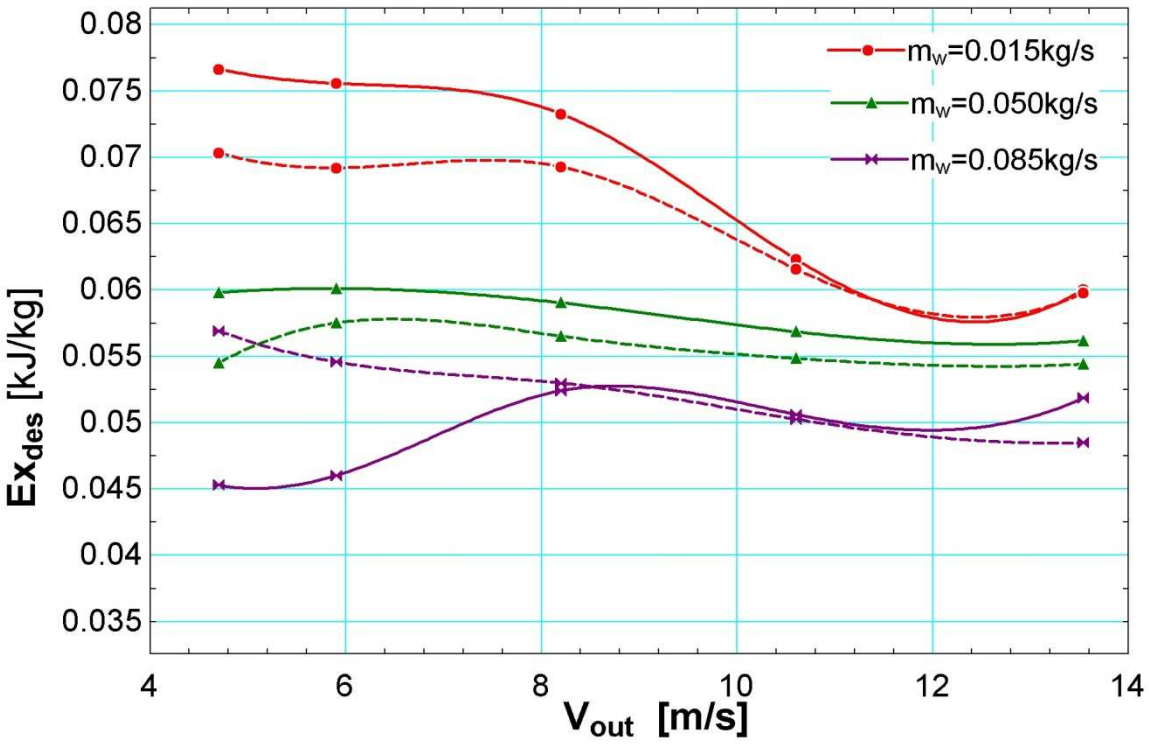


**Figure 6.22 Variation of exergy destruction with air velocity at different water flow rates**

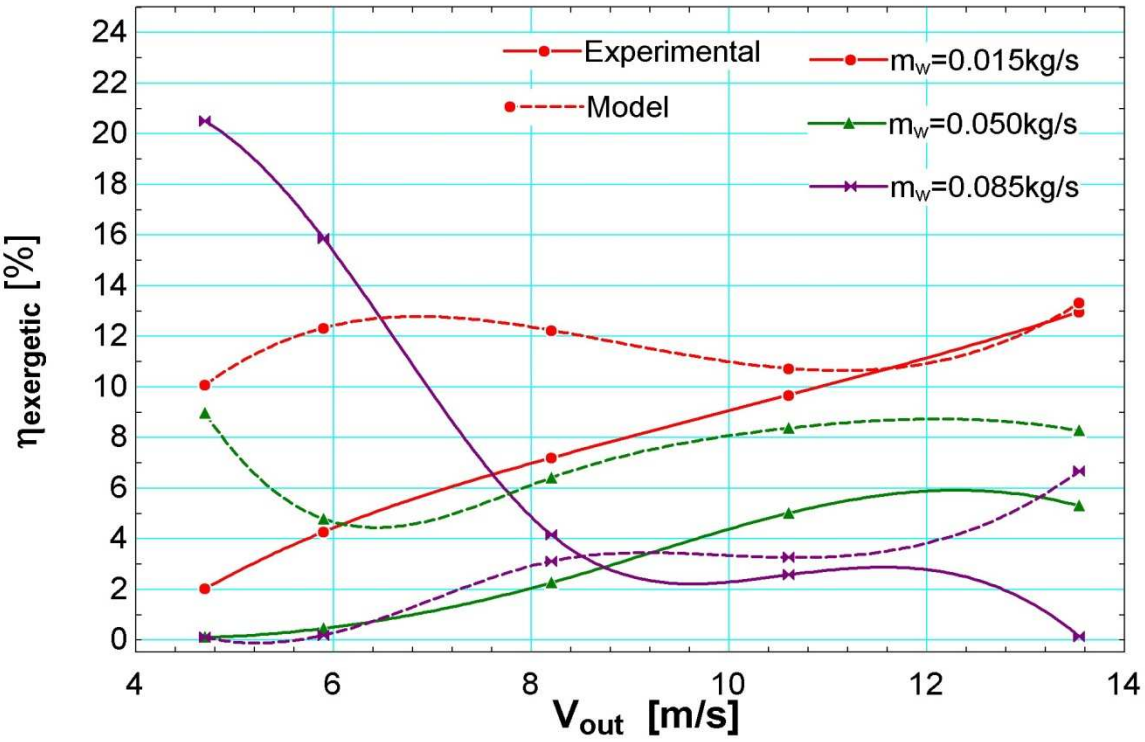


**Figure 6.23 Variation of exergetic efficiency with air velocity at different water flow rates**

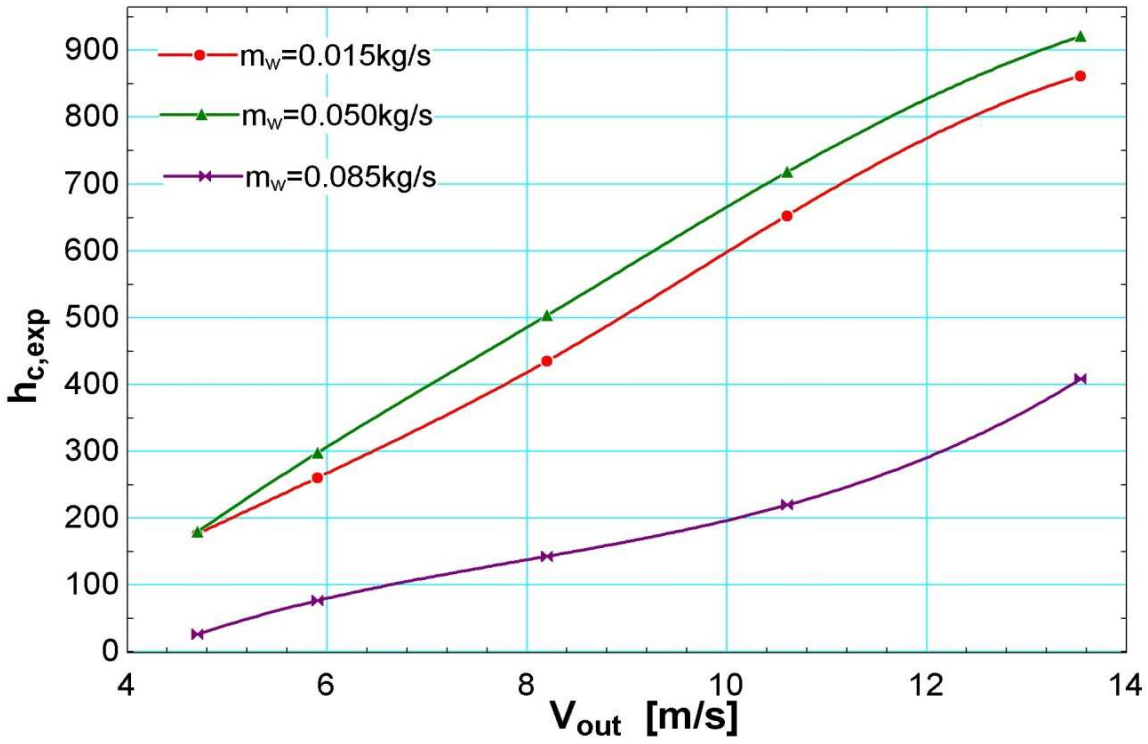


**Figure 6.24 Variation of heat transfer coefficient with Velocity of air at different water flow rates**

### 6.3 Chilled water temperature:

The temperature of inlet water to the wet cooling media is in the range of 5 to $9^0$C, whereas that of environmental incoming air is in the range of 26 to $32^0$C. The experimental results show a temperature drop in the range of 4 to $7^0$C, for different air to water flow ratios. The air flow velocities ranging from 4.7 to 13.54m/s, whereas water flow rate ranging from 0.015 to 0.085 kg/s. The increase in temperature of water measured in the range of 15 to $24^0$C. The performance parameters are cooling efficiency, humidifying efficiency, wet bulb effectiveness and dew point effectiveness. Figures 6.25 through 6.34 conclude the performance of the system.

#### 6.3.1 The drop in DBT

The drop in DBT of flowing air measured is more in case of chilled water as compared to that in case of normal water temperature, which is due to the fact that water requires more heat for evaporation.

Figure 6.25 depicts the variation of change in DBT of air with change in velocity of air at different mass flow rates of water. The trend is of decrease in DBT drop with increase in velocity of air, i.e. increase in outlet temperature for same inlet temperature with increase in air velocity, which is due to air to water contact time. It is clear from the figure that change in DBT per unit change in air flow rate is maximum at maximum water flow rate and minimum at minimum water flow rates.. The experimental drop in DBT is from 4-$7^0$C.

#### 6.3.2 Cooling efficiency:

Figure 6.26 depicts the variation of cooling efficiency with change in velocity of air for at different mass flow rates of water. The trend is of decrease in cooling efficiency with increase in velocity of air, which is due to air to water contact time. The experimental cooling efficiency ranges from 60-80%.

**Table 13: Experimental Inlet and outlet dry bulb temperature and relative humidity at chilled water temperature, m_w=0.015 kg/s at different air velocities**

| $M_w$ =0.015 kg/s | | | | | | |
|---|---|---|---|---|---|---|
| $V_a$ (m/s) | $T_{air}$ (DBT $^0$C) | | $T_{water}$($^0$C) | | Rel. Hum. (%) | |
| | IN | OUT | IN | OUT | IN | OUT |
| 4.70 | 32 | 27 | 8 | 24.5 | 57 | 83 |
| 5.90 | 32 | 27.3 | 7 | 25 | 56 | 81 |
| 8.20 | 32.1 | 27.5 | 7 | 25 | 56 | 80 |
| 10.60 | 32.2 | 27.8 | 8 | 25.2 | 57 | 79 |
| 13.54 | 32.3 | 27.1 | 8.2 | 25.5 | 57 | 78 |

**Table 14: Experimental Inlet and outlet dry bulb temperatures and relative humidity at chilled water temperature, m_w=0.050 kg/s at different air velocities**

| $M_w$ =0.050 kg/s | | | | | | |
|---|---|---|---|---|---|---|
| $V_a$ (m/s) | $T_{air}$ (DBT $^0$C) | | $T_{water}$($^0$C) | | Rel. Hum. (%) | |
| | IN | OUT | IN | OUT | IN | OUT |
| 4.70 | 32.1 | 26.9 | 6 | 23.6 | 56 | 78 |
| 5.90 | 32 | 27.1 | 6 | 24 | 56 | 79 |
| 8.20 | 32 | 27.2 | 6 | 24.2 | 57 | 81 |
| 10.60 | 31.9 | 27.3 | 5.5 | 24.4 | 57 | 81 |
| 13.54 | 31.9 | 27.4 | 6 | 24.9 | 57 | 81 |

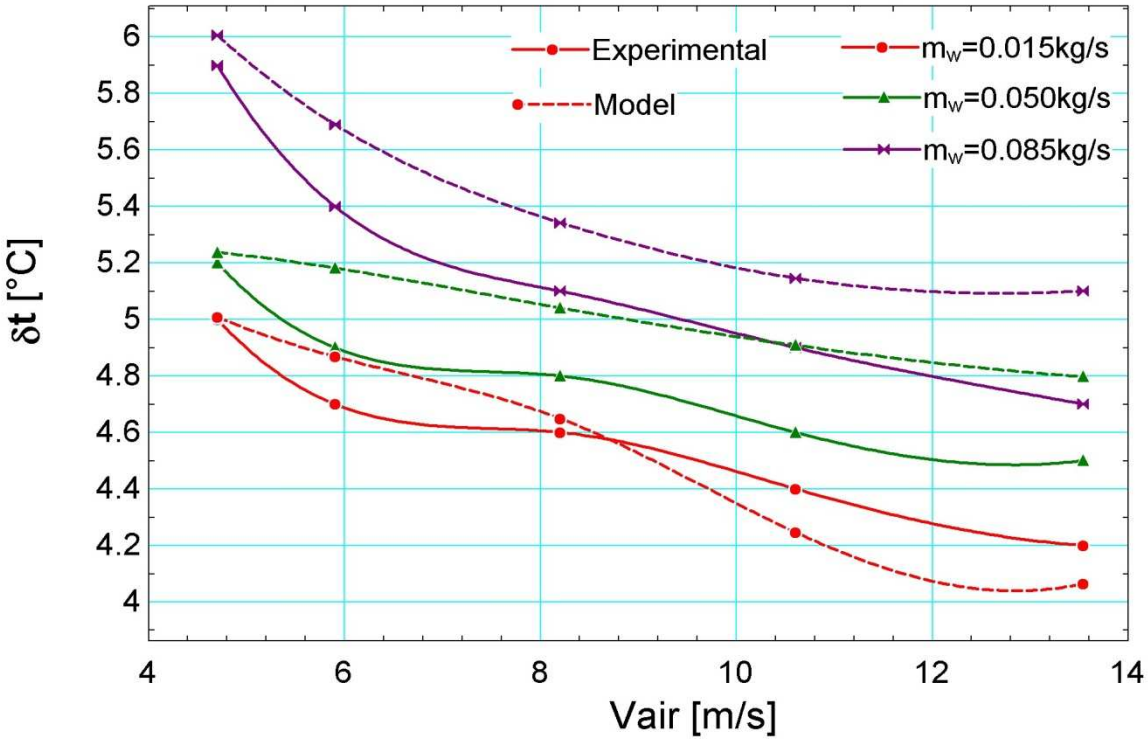


**Figure 6.25 Variation of temperature drop with Air velocity for chilled water at different water flow rates**

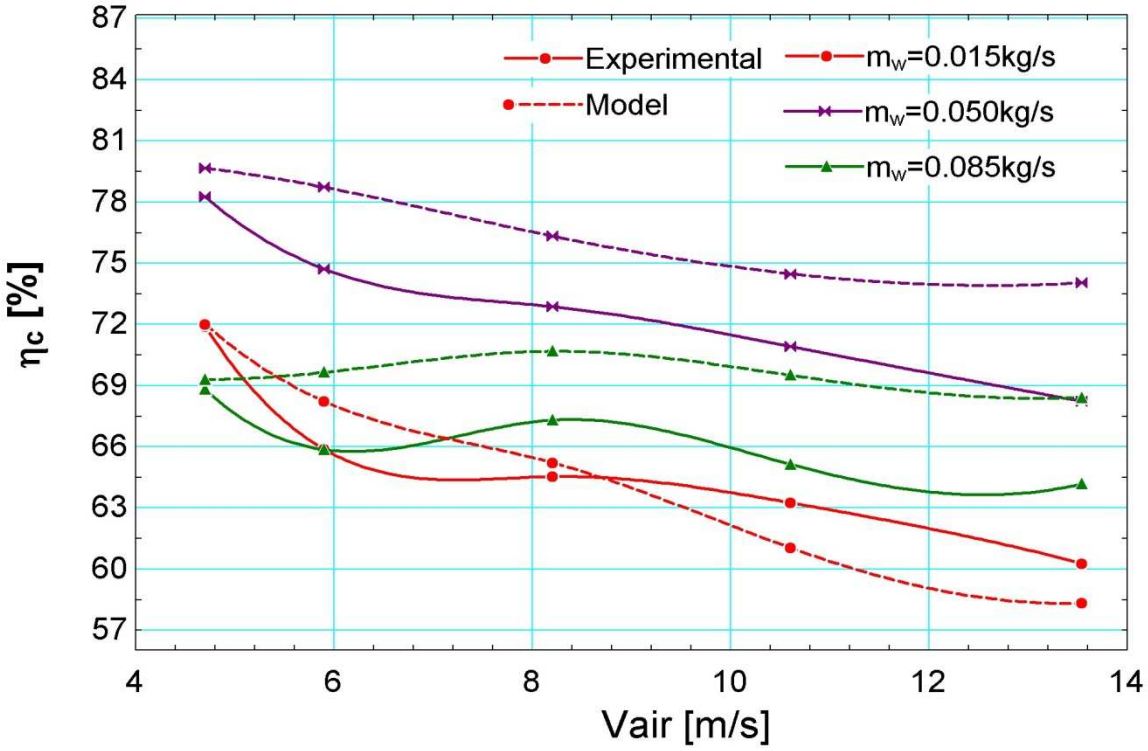


**Figure 6.26 Variation of cooling efficiency with Air velocity for chilled water at different water flow rates**

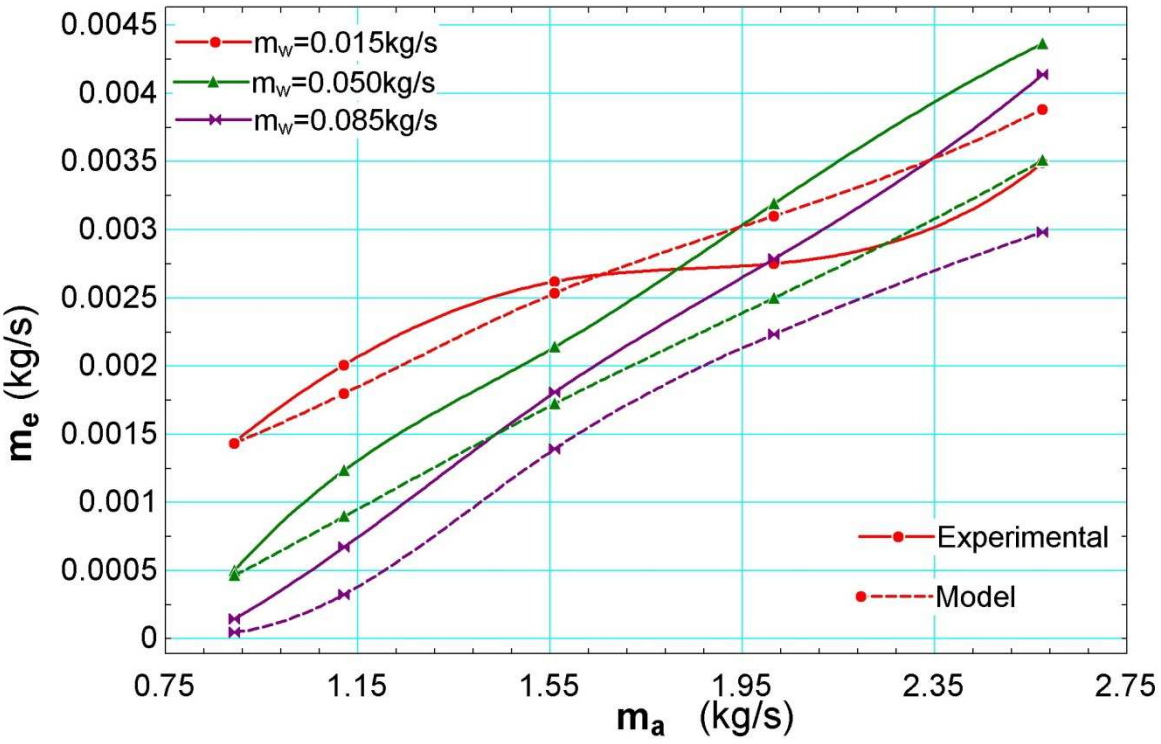


**Figure 6.27 Variation of water evaporation rate with mass of air at different water flow rates**

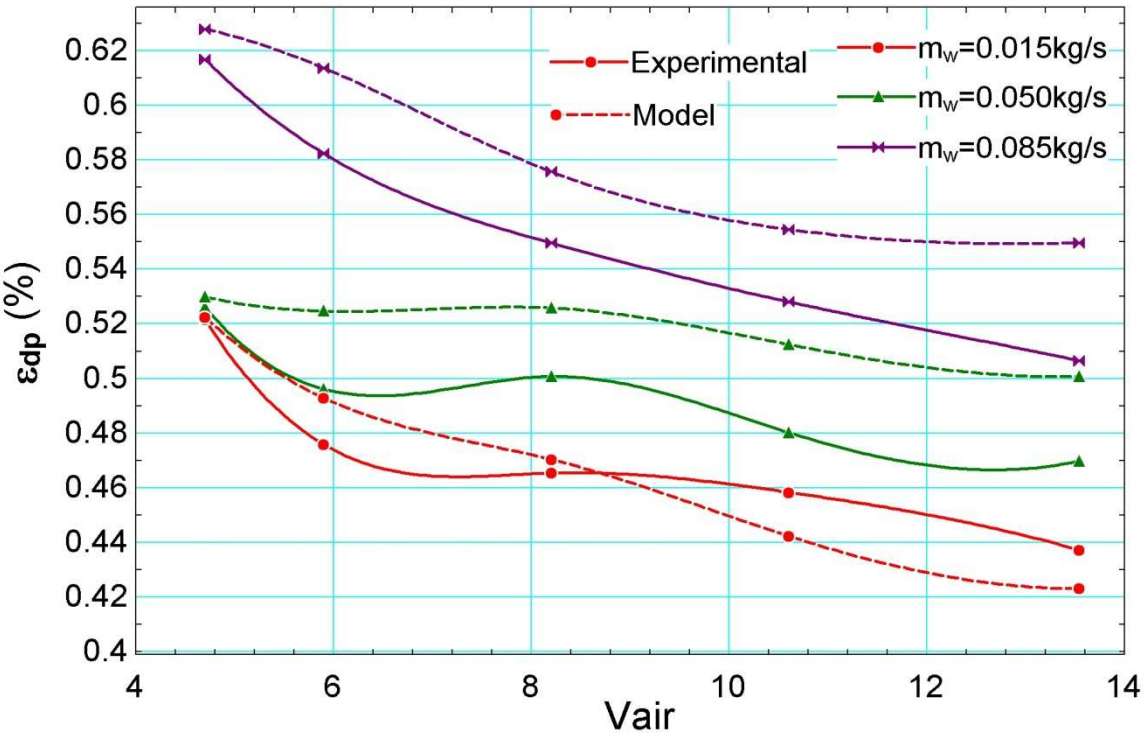


**Figure 6.28 Variation of dew point effectiveness with Air velocity at different water flow rates**

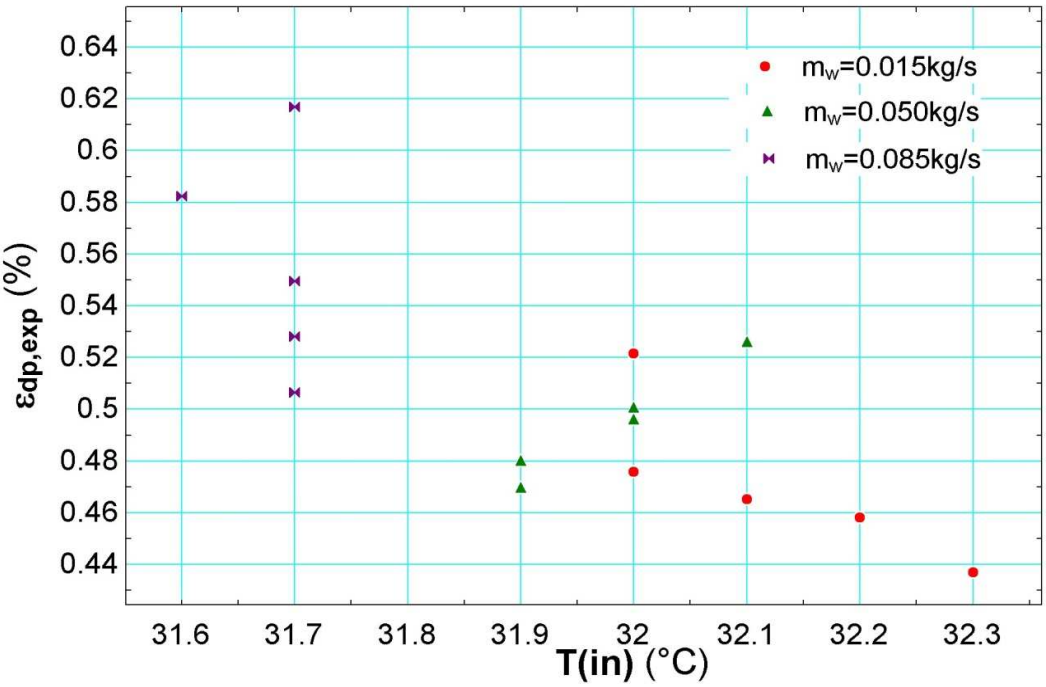


**Figure 6.29 Variation of dew point effectiveness with Air inlet temperature at different water flow rates**

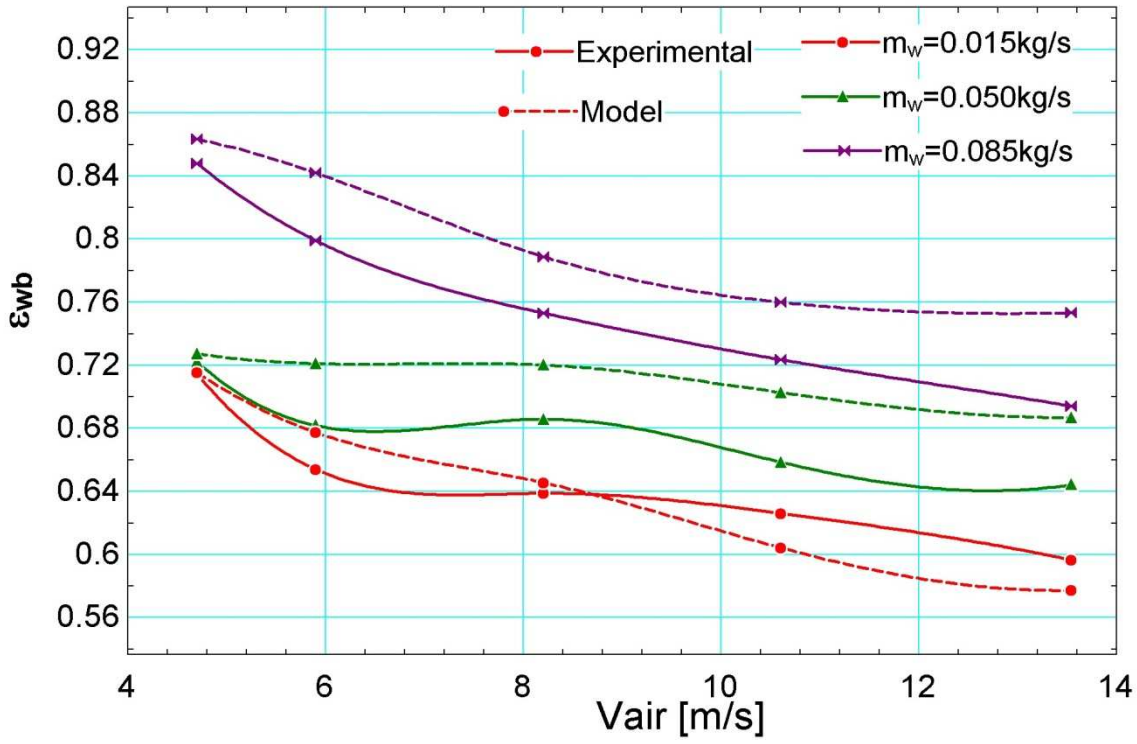


**Figure 6.30 Variation of dew point effectiveness with Air velocity at different water flow rates**

**Table 15: Experimental Inlet and outlet dry bulb temperature and relative humidity at Chilled water temperature, m_w=0.085 kg/s at different air velocities**

| $M_w$ =0.085 kg/s | | | | | | |
|---|---|---|---|---|---|---|
| $V_a$ (m/s) | $T_{air}$ (DBT $^0$C) | | $T_{water}$($^0$C) | | Rel. Hum. (%) | |
| | IN | OUT | IN | OUT | IN | OUT |
| 4.70 | 31.7 | 25.8 | 5 | 20.3 | 57 | 81 |
| 5.90 | 31.6 | 26.2 | 5.1 | 21.4 | 58 | 82 |
| 8.20 | 31.7 | 26.6 | 9.5 | 24 | 58 | 83 |
| 10.60 | 31.7 | 26.8 | 8.8 | 23.3 | 58 | 83 |
| 13.54 | 31.7 | 27 | 6.9 | 24.1 | 58 | 82 |

**Table 16: Comparison of Experimental and model data for chilled water temperature m_w=0.015 kg/s at different air velocities**

| $M_w$ =0.015 kg/s | | | | | | | | |
|---|---|---|---|---|---|---|---|---|
| $V_a$ (m/s) | $T_{air,in}$ (DBT$^0$C) | Rel. $Hum._{in}$ (%) | $T_{air,out}$(DBT$^0$C) | | | Rel. $Hum._{out}$ (%) | | |
| | | | Model | Experimental | Difference | Model | Experiment | Difference |
| 4.70 | 32 | 57 | 26.99 | 27 | 0.01 | 80 | 83 | 3 |
| 5.90 | 32 | 56 | 27.13 | 27.3 | 0.87 | 79 | 81 | 2 |
| 8.20 | 32.1 | 56 | 27.45 | 27.5 | 0.05 | 77 | 80 | 3 |
| 10.60 | 32.2 | 57 | 27.95 | 27.8 | -0.15 | 75 | 79 | 4 |
| 13.54 | 32.3 | 57 | 28.24 | 28.1 | -0.14 | 74 | 78 | 4 |

**Table 17: Comparison of Experimental and model data for chilled water temperature m_w=0.050 kg/s at different air velocities**

| $M_w$ =0.050 kg/s | | | | | | | | |
|---|---|---|---|---|---|---|---|---|
| $V_a$ (m/s) | $T_{air,in}$ ($DBT^0C$) | Rel. $Hum._{in}$ (%) | $T_{air,out}$($DBT^0C$) | | | Rel. $Hum._{out}$ (%) | | |
| | | | Model | Experimental | Difference | Model | Experiment | Difference |
| 4.70 | 32.1 | 56 | 26.86 | 26.9 | 0.04 | 75 | 78 | 3 |
| 5.90 | 32 | 56 | 26.82 | 27.1 | 0.28 | 76 | 79 | 3 |
| 8.20 | 32 | 57 | 26.96 | 27.2 | 0..24 | 79 | 81 | 2 |
| 10.60 | 31.9 | 57 | 26.99 | 27.3 | 0.31 | 80 | 81 | 1 |
| 13.54 | 31.9 | 57 | 27.1 | 27.4 | 0.30 | 80 | 81 | 1 |

**Table 18: Comparison of Experimental and model data for chilled water temperature m_w=0.085 kg/s at different air velocities**

| $M_w$ =0.085 kg/s | | | | | | | | |
|---|---|---|---|---|---|---|---|---|
| $V_a$ (m/s) | $T_{air,in}$ ($DBT^0C$) | Rel. $Hum._{in}$ (%) | $T_{air,out}$($DBT^0C$) | | | Rel. $Hum._{out}$ (%) | | |
| | | | Model | Experimental | Difference | Model | Experiment | Difference |
| 4.70 | 31.7 | 57 | 25.69 | 25.8 | 0.11 | 81 | 81 | 0 |
| 5.90 | 31.6 | 58 | 25.91 | 26.2 | 0.29 | 80 | 82 | 2 |
| 8.20 | 31.7 | 58 | 26.36 | 26.6 | 0.24 | 81 | 83 | 2 |
| 10.60 | 31.7 | 58 | 26.55 | 26.8 | 0.25 | 81 | 83 | 2 |
| 13.54 | 31.7 | 58 | 26.6 | 27 | 0.4 | 82 | 83 | 1 |

Figure 6.27 depicts the variation in Water evaporation rate with change in air flow rate at different water flow rates. The trend is of increase water evaporation rate with increase in air flow rate, which is due to more and more mass flow rate of air. Water evaporation rate shows very less variation with water flow rate.

### 6.3.3 Dew point effectiveness:

Figure 6.28 depicts the variation in dew point effectiveness with change in air velocities at different water flow rates. The trend is of decrease in dew point effectiveness with increase in air velocity, which is due to less and less time of contact of air with water with higher air velocities. The fit used in the diagram is cubic fit, which deviates from the trend, at some instants which is due to change in inlet air conditions. The experimental dew point effectiveness varies from 0.4 to 0.6.

Figure 6.29 depicts comparison of experimental dew point effectiveness versus model results at different water flow rates. The results shown in figure depict very less deviation of experimental results from that one of the model.

### 6.3.4 Wet bulb effectiveness:

Figure 6.30 depicts the variation in wet bulb effectiveness with change in air velocities at different water flow rates. The trend is of decrease in wet bulb effectiveness with increase in velocity, which is due to less and less time of contact of air with water with higher air velocities. The experimental wet bulb effectiveness ranges from 0.60 to 0.85.

Figure 6.31 depicts variation of wet bulb effectiveness with Inlet air temperature at different water flow rates. The trend is of decreased wet bulb effectiveness with increase in temperature. Results shown in figure depict very less deviation of experimental results from that one of the model.

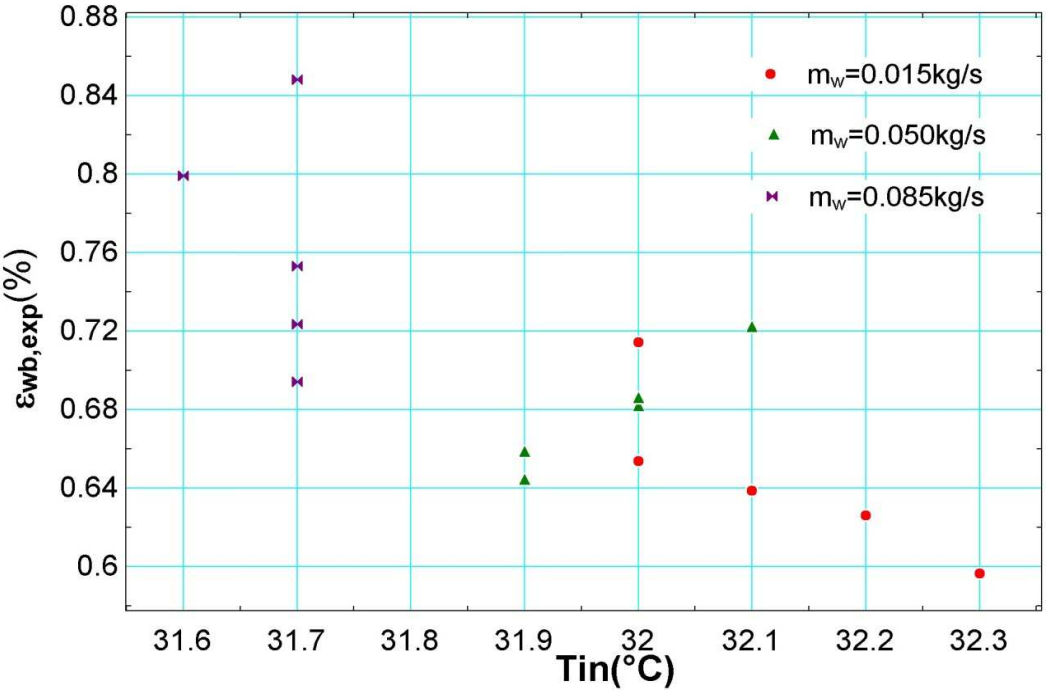


**Figure 6.31 Variation of Wet bulb effectiveness with Air inlet temperature at different water flow rates**

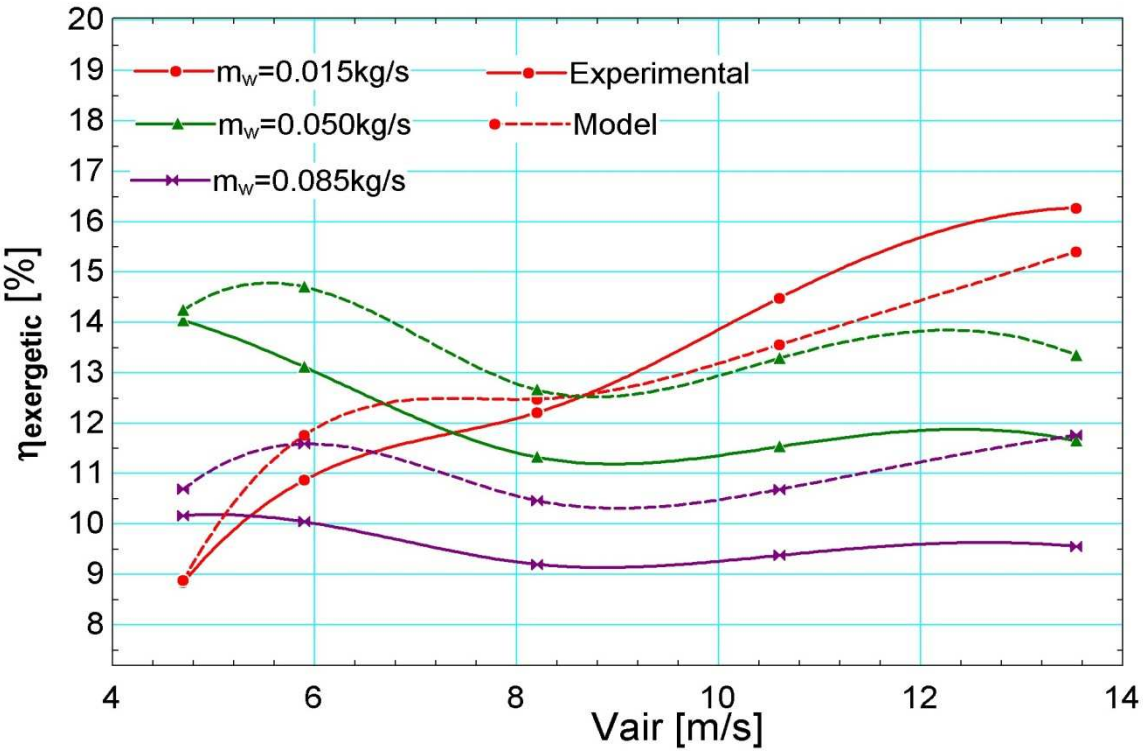


**Figure 6.32 Variation of exergetic efficiency with velocity at different water flow rates**

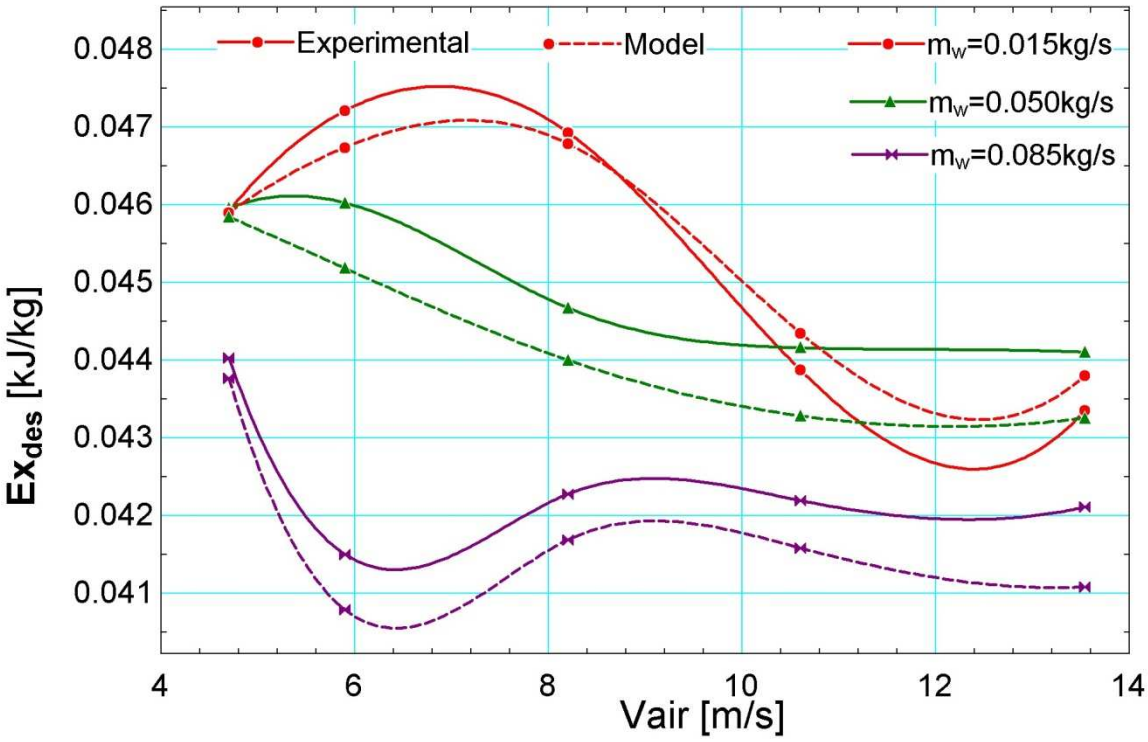


**Figure 6.33 Variation of exergy destruction with velocity at different water flow rates**

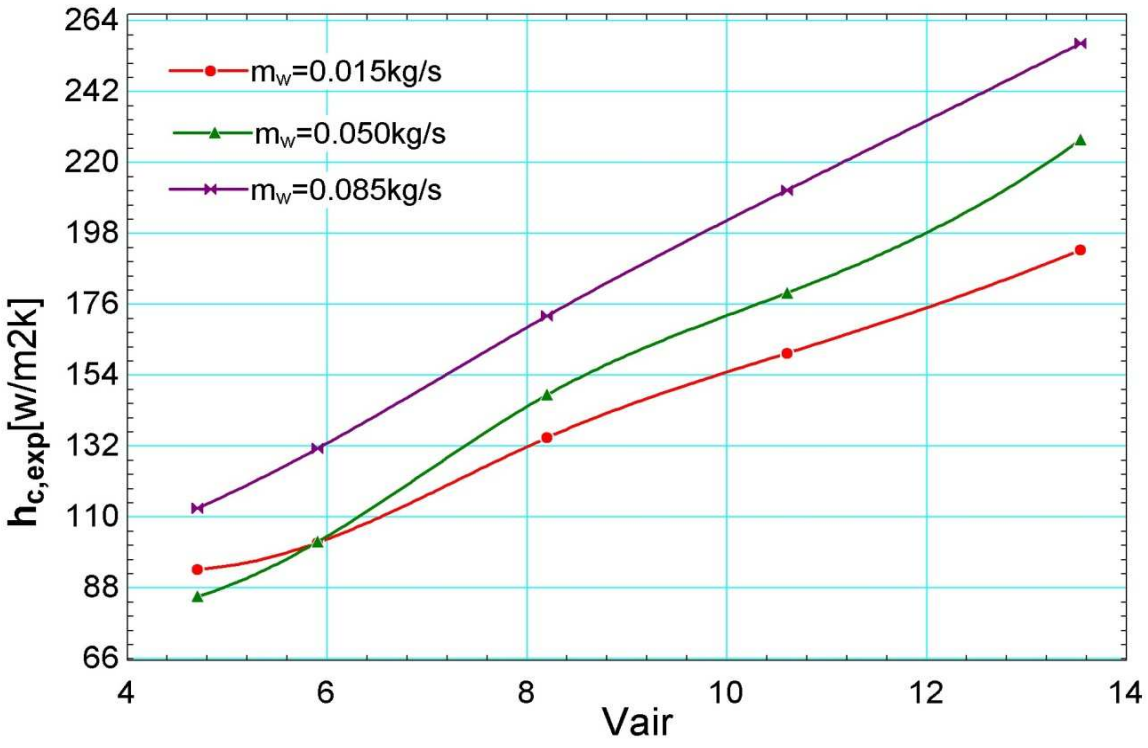


**Figure 6.34 Variation of heat transfer coefficient with velocity of air at different water flow rates**

### 6.3.5 Exergy destruction and exergetic efficiency:

There is a destruction of exergy of the flowing air in evaporative cooling systems. The graphs 6.32 through 6.33 show the variation of exergy destruction and exergetic efficiency with variation of velocity of air. The deviation from trend is due to variation in the inlet conditions of air.

### 6.3.6 Heat transfer coefficient:

Heat transfer coefficient increases with increase in velocity of air as is obvious from figure 6.34. Heat transfer coefficient is a function of velocity of air and mean temperature of the air. It also increases with increase in mass flow rate of water.

# Chapter 7

# Conclusions and Recommendations

Evaporative cooling of air and water is utilized in various industrial, agricultural and domestic purposes in India and other parts of country. The major benefit of using evaporative cooling is use of potential of air itself to absorb water to cool itself and flowing water along with. The major **conclusions** drawn from the chapter number 6, results and discussion are:

1. The evaporative cooling of air, if water used is at normal temperature i.e. between DBT and WBT of air, a sufficient amount of temperature drop is achieved with an average cooling efficiency of around 40%. The temperature of water drops down by around $2^0$C. The practical example of this case is dessert cooler.
2. If the water used is at a temperature very much lower than the WBT of air, the cooling of air achieved is more, of the order of around $7^0$C whereas water gets heated through around $20^0$C.
3. If water used is at elevated temperatures above DBT of air (46-52$^0$C), the drop in air temperature is less, of the order of around $3^0$C, whereas the water temperature drops by about $20^0$C. This is the case of cross flow cooling tower.
4. The velocity of air impacts greatly each of the performance parameters, in all the three cases discussed above.
5. Mass flow rate of water flowing through the cooling media also impacts the performance parameters in all the three cases, as is also discussed in the results and discussion of the present work.
6. The heat transfer coefficients of various studied, varies mainly with the mean temperature of air flow and velocity of the air.

## Recommendations:

The major drawback of evaporative cooling systems is that the cooling is directly linked with evaporation of water hence it more evaporation more cooling therefore the outlet humidity goes on increasing with less outlet temperature. Hence improvements are needed for humidity control of outlet air, which can be done by dehumidifiers used in direct evaporative coolers or the use of indirect evaporative coolers.

## References


[1] M.F. El-Refaie, S. Kaseb ***"Speculation in the feasibility of evaporative cooling",*** Building and Environment, 44 (2009) 826–838

[2] Yunus cerci, *"**A new ideal evaporative freezing cycle",*** International Journal of Heat and Mass Transfer 46 (2003) 2967–2974

[3] P. STABAT, D. MARCHIO ***"Limits of feasibility and energy consumption of desiccant and evaporative cooling in temperate climates"*** ,Centre for energy studies, France

[4] Renato M. Lazzarin***" Introduction of a simple diagram-based method for analyzing evaporative cooling"*** Applied Thermal Engineering 27 (2007) 2011–2025

[5] Ghassem Heidarinejad , Mohammad Heidarinejad , Shahram Delfani , Jafar Esmaeelian "***Feasibility of using various kinds of cooling systems in a multi-climates country",*** Energy and Buildings 40 (2008) 1946–1953

[6] Ren Chengqin, Li Nianping, Tang Guangfa ***"Principles of exergy analysis in HVAC and evaluation of evaporative cooling schemes"*** Building and Environment 37 (2002) 1045 – 1055

[7] M.S. Sodha, S.P. Singh, R.L. sawhney ***"Evolution of design patterns for direct evaporative coolers"*** Pergamon- 0360-1323-(94)00034-41

[8] Robert E. Foster *"**Evaporative air-conditioning contributions to reducing greenhouse Gas emissions and global warming"*** New Mexico State University

[9] Jose´ Rui Camargo, Carlos Daniel Ebinuma, Jose´ Luz Silveira ***"Experimental performance of a direct evaporative cooler operating during summer in a Brazilian city"*** International Journal of Refrigeration 28 (2005) 1124–1132

[10] Carla Fernanda Barbosa Teixeira, Lucila Chebel Labaki ***"Evaporative Cooling in Tropical Climate:Case Study of Campinas, Brazil"*** PLEA2006 - The 23rd Conference on

Passive and Low Energy Architecture, Geneva, Switzerland, 6-8 September 2006

[11] Ebrahim Hajidavalloo***," Application of evaporative cooling on the condenser of window air-conditioner",*** Applied Thermal Engineering 27 (2007) 1937–1943

[12] Marcos B. Bellorio, Joao M.D.Pimenta, ***"Theoritical analysis of air conditioning by evaporative cooling influence on gas turbine cycle performance"*** 18th international congress of mechanical engineering November 06-11, 2005, Ouro Preto MG

[13] João M. D. Pimenta, Wagner P. De Castro **"Analysis of different applications of evaporative cooling systems"**

[14] M. Maerefat*, A.P. Haghighi ***"Natural cooling of stand-alone houses using solar Chimney and evaporative cooling cavity",*** Renewable Energy 35 (2010) 2040–2052

[15] Ebrahim Hajidavalloo***," Application of evaporative cooling on the condenser of window air-conditioner",*** Applied Thermal Engineering 27 (2007) 1937–1943

[16] Khalid A. Joudi, Salah M. Mehdi ***"Application of indirect evaporative cooling to variable domestic cooling load"*** *Energy Conversion & Management 41 (2000) 1931-1951*

[17] C. Kutscher D. Costenaro *"**Assessment of Evaporative Cooling Enhancement Methods for Air-Cooled Geothermal Power Plants"*** presented at the Geothermal Resources Council (GRC) Annual Meeting Reno, Nevada September 22−25, 2002

[18] E.E. Anyanwu **"Design and measured performance of a porous evaporative cooler for preservation of fruits and vegetables"** Energy Conversion and Management 45 (2004) 2187–2195

[19] Kunxiong Tan, Shiming Deng ***"A numerical analysis of heat and mass transfer inside a reversibly used water cooling tower"*** Building and Environment 38 (2003) 91 – 97

[20] B.N. Taufiq, H.H. Masjuki, T.M.I. Mahlia, M.A. Amalina, M.S. Faizul, R. Saidur ***"Exergy analysis of evaporative cooling for reducing energy use in a Malaysian building"*** Desalination 209 (2007) 238–243

[21] Ren Chengqina, Li Nianpingb, Tang Guangfab ***"Principles of exergy analysis in HVAC and evaluation of evaporative cooling schemes"*** Building and Environment 37 (2002) 1045 – 1055

[22] J.M.Wu, X. Huang, H. Zhang ***" Theoretical analysis on heat and mass transfer in a direct evaporative cooler"*** Applied thermal engineering

[23] J.M.Wu, X. Huang, H. Zhang ***" Numerical investigation on heat and mass transfer in a direct evaporative cooler"*** Applied thermal engineering

[24] Ala Hasan ***"Indirect evaporative cooling of air to a sub-wet bulb temperature"*** Applied Thermal Engineering xxx (2010) 1-9

[25] J.A.Dowdy, J.A.Bryant***, "Performance of a rigid cellulose evaporative medium for elevated inlet water temperatures"*** ASHRAE Transactions Research

[26] B. Riangvilaikul, S. Kumar ***"An experimental study of a novel dew point evaporative cooling system"*** Energy and Buildings 42 (2010) 637–644

[27] R. Sureshkumar, S.R. Kale , P.L. Dhar ***"Heat and mass transfer processes between a water spray and ambient air – II. Simulations"*** Applied Thermal Engineering 28 (2008) 361–371

[28] A.S. Kaiser,M. Lucas, A. Viedma b Zamora***" Numerical model of evaporative cooling processes in a new type of cooling tower"*** International Journal of Heat and Mass Transfer 48 (2005) 986–999

[29] Y.J. Dai, K. Sumathy ***"Theoretical study on a cross-flow direct evaporative cooler using honeycomb paper as packing material"*** Applied Thermal Engineering 22 (2002) 1417–1430

[30] Chung-Min Liao, Kun-Hung Chiu***" Wind tunnel modelling the system performance of alternative evaporative cooling pads in Taiwan region"*** Building and Environment 37 (2002) 177–187

[31] Boris Halasz ***"Application of a general non-dimensional mathematical model to cooling towers"***, International Journal of thermal science,(1999)38.75-88

[32] Qun Chen , Kangding Yang, Moran Wang , Ning Pan , Zeng-Yuan Guo ***,"A new approach to analysis and optimization of evaporative cooling system I: Theory"*** Energy 35 (2010) 2448-2454

[33] A. Fouda , Z. Melikyan ***" A simplified model for analysis of heat and mass transfer in a direct evaporative cooler"*** Applied Thermal Engineering 31 (2011) 932-936

[34] M. Lemouari , M. Boumaza, A. Kaabi ***"Experimental analysis of heat and mass transfer phenomena in a direct contact evaporative cooling tower"*** Energy Conversion and Management 50 (2009) 1610–1617

[35] R. Sureshkumar, S.R. Kale, P.L. Dhar ***"Heat and mass transfer processes between a water spray and ambient air – I. Experimental data"*** Applied Thermal Engineering 28 (2008) 349–360

[36] B. Costelloe, D.P. Finn ***"Heat transfer correlations for low approach evaporative cooling systems in buildings"*** Applied Thermal Engineering 29 (2009) 105–115

[37] A. Beshkani, R. Hosseini ***"Numerical modeling of rigid media evaporative cooler"*** Applied Thermal Engineering 26 (2006) 636–643

[38] Paisarn Naphon***," Study on the heat transfer characteristics of an evaporative cooling tower"***

[39] Hakan Caliskan, Ibrahim Dincer, Arif Hepbasli ***"Exergetic and sustainability performance comparison of novel and conventional air cooling systems for building applications"***,*Energy and Buildings* (2010)

[40] B.N. Taufiq*, H.H. Masjuki, T.M.I. Mahlia***,"Exergy analysis of evaporative cooling for reducing energy use in a Malaysian"***, Desalination 209 (2007) 238–243

[41] Ren Chengqin, Li Nianping, Tang Guangfa ***"Principles of exergy analysis in HVAC and evaluation of evaporative cooling schemes"*** Building and Environment 37 (2002) 1045 – 1055

42 Yogesh Jaluria, "Design and optimization of thermal systems"-II Edition, CRC press, p-187